

Grading and Interpretation of White Matter Hyperintensities Using Statistical Maps

Wi-Sun Ryu, Sung-Ho Woo, Dawid Schellingerhout, Moo K. Chung, Chi Kyung Kim, Min Uk Jang, Kyoung-Jong Park, Keun-Sik Hong, Sang-Wuk Jeong, Jeong-Yong Na, Ki-Hyun Cho, Joon-Tae Kim, Beom Joon Kim, Moon-Ku Han, Jun Lee, Jae-Kwan Cha, Dae-Hyun Kim, Soo Joo Lee, Youngchai Ko, Yong-Jin Cho, Byung-Chul Lee, Kyung-Ho Yu, Mi-Sun Oh, Jong-Moo Park, Kyusik Kang, Kyung Bok Lee, Tai Hwan Park, Juneyoung Lee, Heung-Kook Choi, Kiwon Lee, Hee-Joon Bae and Dong-Eog Kim

Stroke. 2014;45:3567-3575; originally published online November 11, 2014;
doi: 10.1161/STROKEAHA.114.006662

Stroke is published by the American Heart Association, 7272 Greenville Avenue, Dallas, TX 75231
Copyright © 2014 American Heart Association, Inc. All rights reserved.
Print ISSN: 0039-2499. Online ISSN: 1524-4628

The online version of this article, along with updated information and services, is located on the World Wide Web at:

<http://stroke.ahajournals.org/content/45/12/3567>

Data Supplement (unedited) at:

<http://stroke.ahajournals.org/content/suppl/2014/11/11/STROKEAHA.114.006662.DC1.html>

Permissions: Requests for permissions to reproduce figures, tables, or portions of articles originally published in *Stroke* can be obtained via RightsLink, a service of the Copyright Clearance Center, not the Editorial Office. Once the online version of the published article for which permission is being requested is located, click Request Permissions in the middle column of the Web page under Services. Further information about this process is available in the [Permissions and Rights Question and Answer](#) document.

Reprints: Information about reprints can be found online at:
<http://www.lww.com/reprints>

Subscriptions: Information about subscribing to *Stroke* is online at:
<http://stroke.ahajournals.org/subscriptions/>

Grading and Interpretation of White Matter Hyperintensities Using Statistical Maps

Wi-Sun Ryu, MD, PhD*; Sung-Ho Woo, PhD*; Dawid Schellingerhout, MD; Moo K. Chung, PhD; Chi Kyung Kim, MD; Min Uk Jang, MD; Kyoung-Jong Park, MS; Keun-Sik Hong, MD, PhD; Sang-Wuk Jeong, MD, PhD; Jeong-Yong Na, BS; Ki-Hyun Cho, MD, PhD; Joon-Tae Kim, MD, PhD; Beom Joon Kim, MD, PhD; Moon-Ku Han, MD, PhD; Jun Lee, MD, PhD; Jae-Kwan Cha, MD, PhD; Dae-Hyun Kim, MD, PhD; Soo Joo Lee, MD, PhD; Youngchai Ko, MD; Yong-Jin Cho, MD, PhD; Byung-Chul Lee, MD, PhD; Kyung-Ho Yu, MD, PhD; Mi-Sun Oh, MD, PhD; Jong-Moo Park, MD, PhD; Kyusik Kang, MD, PhD; Kyung Bok Lee, MD, PhD; Tai Hwan Park, MD, PhD; Juneyoung Lee, PhD; Heung-Kook Choi, PhD; Kiwon Lee, MD; Hee-Joon Bae, MD, PhD; Dong-Eog Kim, MD, PhD

Background and Purpose—We aimed to generate rigorous graphical and statistical reference data based on volumetric measurements for assessing the relative severity of white matter hyperintensities (WMHs) in patients with stroke.

Methods—We prospectively mapped WMHs from 2699 patients with first-ever ischemic stroke (mean age=66.8±13.0 years) enrolled consecutively from 11 nationwide stroke centers, from patient (fluid-attenuated-inversion-recovery) MRIs onto a standard brain template set. Using multivariable analyses, we assessed the impact of major (age/hypertension) and minor risk factors on WMH variability.

Results—We have produced a large reference data library showing the location and quantity of WMHs as topographical frequency-volume maps. This easy-to-use graphical reference data set allows the quantitative estimation of the severity of WMH as a percentile rank score. For all patients (median age=69 years), multivariable analysis showed that age, hypertension, atrial fibrillation, and left ventricular hypertrophy were independently associated with increasing WMH (0–9.4%, median=0.6%, of the measured brain volume). For younger (≤69) hypertensives (n=819), age and left ventricular hypertrophy were positively associated with WMH. For older (≥70) hypertensives (n=944), age and cholesterol had positive relationships with WMH, whereas diabetes mellitus, hyperlipidemia, and atrial fibrillation had negative relationships with WMH. For younger nonhypertensives (n=578), age and diabetes mellitus were positively related to WMH. For older nonhypertensives (n=328), only age was positively associated with WMH.

Conclusions—We have generated a novel graphical WMH grading (Kim statistical WMH scoring) system, correlated to risk factors and adjusted for age/hypertension. Further studies are required to confirm whether the combined data set allows grading of WMH burden in individual patients and a tailored patient-specific interpretation in ischemic stroke-related clinical practice. (*Stroke*. 2014;45:3567-3575.)

Key Words: cerebral infarction ■ leukoaraiosis ■ magnetic resonance imaging ■ topographic brain mapping

Received July 4, 2014; final revision received October 2, 2014; accepted October 3, 2014.

From the Stroke Center and Korean Brain MRI Data Center, Dongguk University Ilsan Hospital, Goyang, Korea (W.-S.R., S.-H.W., S.-W.J., J.-Y.N., D.-E.K.); Department of Radiology, University of Texas M. D. Anderson Cancer Center, Houston (D.S.); Department of Biostatistics and Medical Informatics, University of Wisconsin-Madison (M.K.C.); WeBace Co, Ltd, Busan, Korea (K.-J.P.); Department of Neurology, Seoul National University Hospital, Seoul, Korea (C.K.K.); Department of Neurology, Chuncheon Sacred Heart Hospital, Chuncheon, Korea (M.U.J.); Department of Neurology, Ilsan Paik Hospital, Goyang, Korea (K.-S.H., Y.-J.C.); Department of Neurology, Chonnam National University Hospital, Gwangju, Korea (K.-H.C., J.-T.K.); Department of Neurology, Seoul National University Bundang Hospital, Seongnam, Korea (B.J.K., M.-K.H., H.-J.B.); Department of Neurology, Yeungnam University Hospital, Daegu, Korea (J.L.); Department of Neurology, Dong-A University Hospital, Busan, Korea (J.-K.C., D.-H.K.); Department of Neurology, Eulji University Hospital, Daejeon, Korea (S.J.L., Y.K.); Department of Neurology, Hallym University Sacred Heart Hospital, Anyang, Korea (B.-C.L., K.-H.Y., M.-S.O.); Department of Neurology, Eulji General Hospital, Seoul, Korea (J.-M.P., K.K.); Department of Neurology, Soonchunhyang University Hospital, Seoul, Korea (K.B.L.); Department of Neurology, Seoul Medical Center, Seoul, Korea (T.H.P.); Department of Biostatistics, Korea University College of Medicine, Seoul, Korea (J.L.); Department of Computer Science, Inje University, Busan, Korea (H.-K.C.); and Departments of Neurology and Neurosurgery, The University of Texas Health Science Center, Houston (K.L.).

*Drs Ryu and Woo contributed equally.

The online-only Data Supplement is available with this article at <http://stroke.ahajournals.org/lookup/suppl/doi:10.1161/STROKEAHA.114.006662/-/DC1>.

Correspondence to Dong-Eog Kim, MD, PhD, Department of Neurology, Dongguk University Ilsan Hospital, 814 Siksa-dong, Goyang-si, Gyeonggi-do, Korea. E-mail kdongeog@duih.org or Hee-Joon Bae, MD, PhD, Department of Neurology, Seoul National University Bundang Hospital, 82 Gumi-ro 173 beon-gil, Bundang-gu, Seongnam-si, Gyeonggi-do, Korea. E-mail braindoc@snu.ac.kr

© 2014 American Heart Association, Inc.

Stroke is available at <http://stroke.ahajournals.org>

DOI: 10.1161/STROKEAHA.114.006662

White matter hyperintensities (WMHs) are frequently observed on MRIs of elderly people.¹ The presence of WMHs seems to more than double the future risk of stroke.²⁻⁴ Known risk factors for WMHs are age and hypertension.^{1,5} Other risk factors such as diabetes mellitus, hyperlipidemia, atrial fibrillation, and smoking were inconsistently reported in the literature and seem less strongly associated with WMHs (Table I in the online-only Data Supplement).^{3,6-10}

Despite a rapidly growing body of knowledge from population studies, substantial variability in WMH volume among individuals with similar cerebrovascular risk factors complicates a tailored interpretation of patient-specific implications of WMHs in daily clinical practice.¹⁰⁻¹² What is lacking is a comprehensive, quantitative study with substantial numbers, and robust methodology, which correlates WMHs to stroke risk factors so that the associations and interplay between risk factors can be better understood. Clinically, there have been no rigorous graphical and statistical reference data available for the individualized estimation of the relative severity (expressed as percentile ranks) of WMH burden adjusted for major risk factors (age/hypertension).

In this study, we have combined (1) a large number of patients representing a contiguous 10-month window sample of a population of 50 million, (2) at an important clinical landmark, the diagnosis of a first ischemic stroke, with (3) a quantitative image-based statistical analysis methodology. We provide an easy-to-use visual grading system for WMH reflecting the statistical prevalence of WMH in the stroke population, demonstrating both WMH volumes and spatial distributions. We also performed multivariable analyses to investigate the impact of major (age and hypertension) and minor risk factors on WMH volumes and distribution.

Materials and Methods

Study Population

This is a prospective multicenter study that involved 11 academic and regional stroke centers in Korea. From May 2011 to February 2012, we consecutively enrolled 2699 patients with first-ever acute ischemic stroke within 7 days after symptom onset (Figure I in the online-only Data Supplement). The institutional review boards of all participating centers approved this study. All patients or their legally authorized representatives provided a written informed consent for study participation.

Clinical Database

Under a standardized protocol,¹³ we prospectively collected demographic data, prior medication history, laboratory data, and the presence of vascular risk factors (Methods in the online-only Data Supplement).

Brain MRI and Quantitative Image Registration

Detailed protocols of MRI and quantitative image registration are provided in the Methods in the online-only Data Supplement. In brief, MRI was performed on 1.5-Tesla ($n=2338$) or 3.0-Tesla ($n=331$) MRI system (Table II in the online-only Data Supplement). As previously reported,^{14,15} in every patient, all fluid-attenuated inversion recovery MRIs (usually 20–26 5 mm thick slices/patient) were converted into a patient-independent quantitative visual format (Figure II in the online-only Data Supplement) using the Montreal Neurological Institute brain template. After normalization of images, each patient's high signal intensity lesions on fluid-attenuated inversion recovery MRIs were

segmented and registered semiautomatically (by research assistants operating Image_QNA,¹⁴ a custom-built software package) onto the brain templates under close supervision by C.K.K. and M.U.J. These 2 vascular neurologists reviewed the translation process by comparing all the source MR images and corresponding postprocessed images on the template set to either confirm that lesions were faithfully translated or not. Results could be redone or adjusted until approved. On final approval, the graphical record was locked down in the database.

WMH volume percentage was calculated as $100 \times \text{total WMH voxel count (in the template)} / \text{total brain parenchymal voxel count (also in the template)}$, both adjusted for differences in slice spacing (ie, slice thickness and interslice gap) between acquisition (fluid-attenuated inversion recovery MR) images and template images (Table III and Figure III in the online-only Data Supplement). A validation study demonstrated a strong linear correlation ($R^2=0.86$) between the volume calculations done in the template space and volume calculations in the original source MR image space (Figure IV in the online-only Data Supplement).

Statistical Anatomic Maps: WMH Frequency-Volume Maps

To display our data as visual maps, we used 3 Montreal Neurological Institute template slices (centered on 5.5 mm, 20.5 mm, and 35 mm on the z axis) representing the levels of Striatocapsular (5.5 ± 5 mm), Corona Radiata (20.5 ± 5 mm), and Centrum Semiovale (35 ± 5 mm) regions, respectively. These slices were chosen on the basis of clinical experience, as being useful in the grading and interpretation of WMH, and are representative visual images of a larger data set comprising the whole brain. In each of these 3 slices, a WMH frequency map was constructed as previously published^{14,16,17} by plotting the frequency of incidence of WMH lesions at each voxel coordinate of the slice as a heat map (Figure 1). To facilitate the use of our data as reference standard for grading purposes of WMH, we plotted the data as frequency-volume maps to show the statistical volume and spatial distribution in a single format, arranged to reflect the percentile distribution of disease in our study population (Figure 1).

Statistical Analysis

Data are presented as mean \pm SD or median (interquartile range). Intergroup differences and bivariate associations were assessed using nonparametric tests because of a skewed distribution of WMH volumes. Multiple linear regression analysis was performed to identify independent risk factors of WMH volume. For more detailed information for the statistical analysis, please see Methods in the online-only Data Supplement.

Results

Patients and WMHs

Table 1 shows the clinical characteristics of 2699 patients at the time of their first-ever ischemic stroke. The mean age was 66.8 ± 13.0 (range, 20–98) years and 59.5% were men. The most common stroke subtype was large artery disease (38.3%). The median National Institutes of Health Stroke Scale score at presentation was 4 (interquartile range, 2–8). WMH volumes ranged from 0% to 9.37% (median 0.61%; interquartile range, 0.30%–1.31%) of the measured brain volume.

The frequency distribution of WMH volumes was skewed to the right; after log-transformation, log-transformed WMH volume ($_{\log} \text{WMHv}$) were close to being normally distributed ($P=0.06$). Not only the skewed distribution but also the well-known age correlation of WMH volumes was well corroborated by the topographical frequency-volume maps and scatter plots for WMHs (Figure 2; Figure V in the online-only Data Supplement).

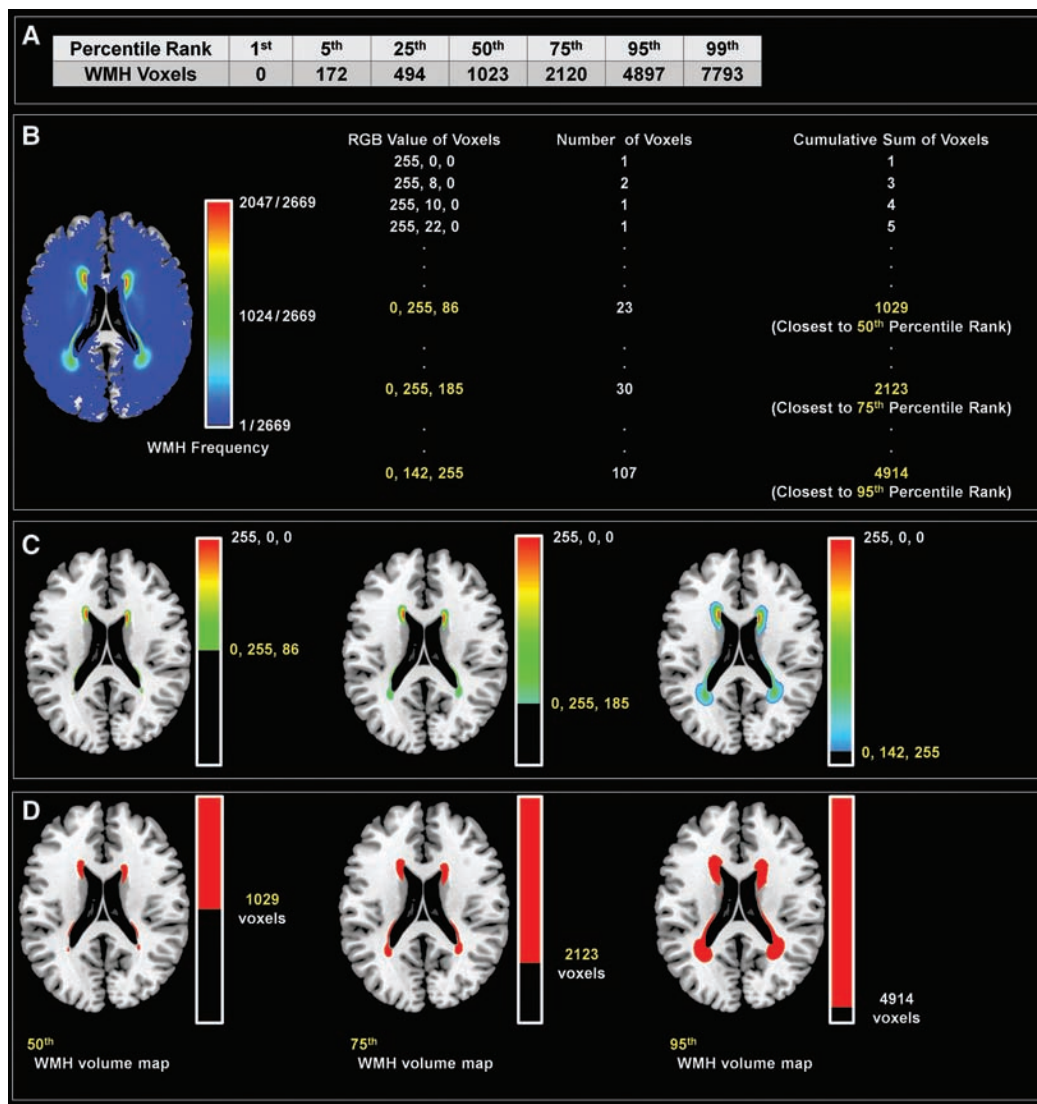


Figure 1. Generating topographical frequency-volume maps to show the statistical volume and spatial distribution of white matter hyperintensities (WMH) in a single format. **A**, Determining percentile values. The number of voxels involved in 2669 consecutive patients with first-ever ischemic stroke are listed in rank order and assigned a percentile value based on their position in the list. In this case, at the 50, 75, and 95 percentiles, there are 1023, 2120, and 4897 voxels abnormal, respectively. Generating frequency maps (**B**) and frequency-volume maps (**B–D**). A custom-built software package (Image_QNA)¹⁴ is used to generate a color-coded WMH frequency map, which is coded into a color to reflect the number of patients who have a lesion in each voxel (**B**). Voxels in the color-coded area of the frequency map are collected in the order of their RGB (Red Green Blue) values ([255, 0, 0]→[0, 255, 0]→[0, 0, 255]) until the total voxel count reaches the number closest to each of the percentile values of WMH voxel counts (**B** and **C**). The other unselected voxels are made transparent (**C**). The selected voxels are highlighted as red-color overlays (**D**).

Frequency-Volume Maps

Figure 2 shows the results of a combined mapping of both spatial location and frequency of occurrence of WMH lesions. Figure 2A demonstrates with color-coded maps the location and incidence of WMH in the entire patient study population. In Figure 2B, an alternate display technique is used to indicate the percentiles of WMH incidence on all the patients in the study. In Figure 2C, percentile results are broken down by age group, allowing comparison and grading of individual patients to an age-matched cohort. The age stratum-specific topographical frequency-volume maps for WMHs showed that WMH volume on each percentile map gradually increased with increasing age. In addition, the appearance or gradual expansion of WMHs predominantly

occurred around the anterior and posterior horns of the lateral ventricle.

Associations Between WMH Volume and Risk Factors

Bivariate analyses (Table 2) showed that age (Figure V in the online-only Data Supplement), sex, hypertension, left ventricular hypertrophy (LVH), prior use of antiplatelet, atrial fibrillation, smoking, and body mass index were all related to WMH volume. Multiple linear regression analysis showed that age ($\beta=0.500, P<0.01$), hypertension ($\beta=0.089, P<0.01$), and LVH ($\beta=0.055, P=0.01$) had an independent positive relationship with \log_{10} WMHv (Table 2, right). In contrast, atrial fibrillation ($\beta=-0.072, P<0.01$) had an

Table 1. Clinical Characteristics of 2669 Patients With First-Ever Acute Ischemic Stroke

Characteristic	First-Ever Stroke (n=2669)*
Age, y	66.8±13.0
Sex, men	1589 (59.5%)
Hypertension	1763 (66.1%)
Diabetes mellitus	847 (31.7%)
Hyperlipidemia	927 (34.7%)
Smoking, current or quit <5 y	1115 (41.8%)
Atrial fibrillation	543 (20.3%)
Coronary artery disease	311 (11.7%)
Body mass index, kg/m ²	23.6±3.3
Prior use of antiplatelet	584 (21.9%)
Prior use of statin	273 (10.2%)
Stroke subtype	
Large artery disease	1012 (38.3%)
Small vessel occlusion	454 (17.2%)
Cardioembolism	550 (20.8%)
Undetermined	564 (21.4%)
Other determined	61 (2.3%)
NIHSS, median (IQR)	4 (2–8)
Left ventricular hypertrophy	354 (13.3%)
Total cholesterol, mmol/L	4.66±1.08
HDL cholesterol, mmol/L	1.15±0.32
LDL cholesterol, mmol/L	2.93±0.95
Hemoglobin, g/dL	13.6±2.0
Glucose, mmol/L	6.41±2.56
HbA1c, %	6.47±1.46
Systolic blood pressure	145±27
Diastolic blood pressure	86±16
WMH volume (percent of brain volume), median (IQR)	0.61† (0.30–1.31)

HbA1c indicates hemoglobin A1c; HDL, high-density lipoprotein; IQR, interquartile range; LDL, low-density lipoprotein; NIHSS, National Institutes of Health Stroke Scale; and WMH, white matter hyperintensity.

*Data are presented as n (%) or mean±SD.

†WMH volumes were not statistically different between the 1.5-Tesla and 3-Tesla MRI scanners ($P=0.61$, Figure VIII in the online-only Data Supplement), although, for unclear reasons, the clinical characteristics of the patients differed somewhat between these groups (Table VIII in the online-only Data Supplement).

independent negative relationship with \log_{10} WMHv. Sex, prior use of antiplatelet, body mass index, and smoking were not significantly associated with \log_{10} WMHv. After adjusting for participating centers, these associations were unchanged (data not shown).

Age-adjusted \log_{10} WMHv was higher in patients with stroke because of small vessel occlusion (SVO, $n=454$) than in patients ($n=2126$) with other stroke subtypes (Figure VI in the online-only Data Supplement). In the SVO subgroup compared with the non-SVO subgroup, the presence of hypertension had a higher standardized coefficient (0.13 versus 0.07; Results and Table IV in the online-only Data Supplement), suggesting a differentially higher impact of hypertension on the increase of WMH volume in the SVO subgroup than in the

non-SVO subgroup. In contrast, the standardized coefficients for age in both subgroups were similar (0.50 versus 0.49).

Analyses After 2-by-2 Stratification by Hypertension and Age (≤ 69 Versus ≥ 70)

There was a significant interaction between hypertension and age ($P<0.01$; Figure VII in the online-only Data Supplement). Age/hypertension-stratified frequency-volume maps (Figure 3A) showed that WMH volumes appeared to be the highest in the older hypertensive, followed by the older nonhypertensive, younger hypertensive, and then younger nonhypertensive. Statistical parametric mapping further elucidated the age- and hypertension-related effects on WMH volume and distribution (Figure 3B; Results in the online-only Data Supplement).

Multiple linear regression analysis identified subgroup-specific predictors of \log_{10} WMHv (Figure 3C). In the younger patients with hypertension, age and LVH were independently related to \log_{10} WMHv. In the older patients with hypertension, age and cholesterol had a positive relationship with \log_{10} WMHv. However, diabetes mellitus, hyperlipidemia, and atrial fibrillation were negatively associated with \log_{10} WMHv. In the younger nonhypertensive patients, age and diabetes mellitus were positively related to \log_{10} WMHv. In the older nonhypertensive patients, only age was independently associated with \log_{10} WMHv. Further adjustment for the prior use of statins did not change the above results, except that the associations of cholesterol, hyperlipidemia, and diabetes mellitus with \log_{10} WMHv lost significance in the older hypertensive patients (Table V in the online-only Data Supplement). In addition, prior statin use was inversely associated with \log_{10} WMHv in the older nonhypertensive patients ($\beta=-0.149$; $P=0.01$).

Discussion

In this nationwide prospective multicenter study, we have generated topographical frequency-volume maps for WMHs using the entire fluid-attenuated inversion recovery MRI data sets of 2699 consecutive patients with first-ever ischemic stroke. This large statistical sample, presented graphically as statistical maps, provides an objective and quantitative grading (Kim statistical WMH scoring) system for WMH. This, to our knowledge, represents the largest study on WMH mapping and quantification done to date, and the only such study taken at the clinically relevant life event of first ischemic stroke.

We specifically chose patients with first-time stroke, at the time of their first stroke, and excluded from the imaging volumes any WMH attributable to the infarct itself, to obtain a picture of the disease course of WMH right up to the moment of a cerebrovascular incident. Further studies, in different populations, are warranted to test if the new grading system is actually useful as a clinically applicable (Movie in the online-only Data Supplement) imaging reference standard for a patient-specific interpretation in WMH. The value of the grading system as a predictor for stroke risk, for example, is an obvious (though as yet unproven) hypothesis that would need verification in future trials, and in more general populations.

Considering that the reported mean brain volume of an elderly Korean population was 1170 cm³,¹⁸ the median WMH

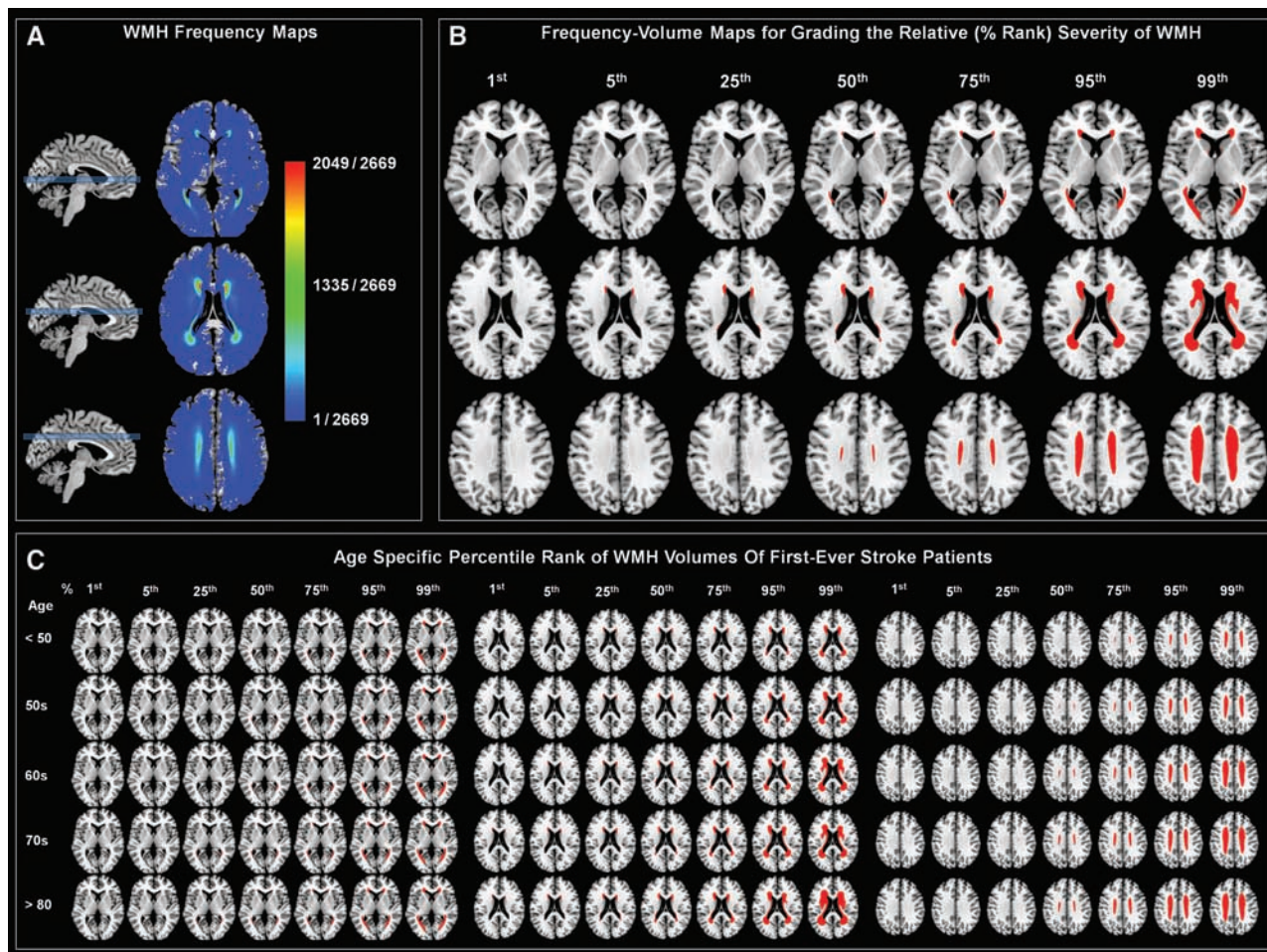


Figure 2. Topographical frequency-volume maps for grading the relative severity (percentile rank) of white matter hyperintensities (WMHs). **A** and **B**, In all 2669 consecutive patients with first-ever ischemic stroke, 256 color-coded frequency maps (**A**) and red color-overlaid grading maps (**B**, frequency-volume maps) for WMHs are displayed at 3 representative brain template slices (5.5 mm, 20.5 mm, 35 mm in z axis of Montreal Neurological Institute space). These slices, the Striatocapsular, Corona Radiata, and Centrum Semiovale levels, are listed from top to bottom in 3 rows, with percentile severity increasing to the right. **C**, Age stratum-specific WMH frequency-volume maps show the age-dependence of WMH volume. Please note that the total voxel count in the red color-overlaid areas of each frequency-volume map is equal or close to the designated (1%–99%) percentile value of WMH voxel counts in the overall (**B**) or age-stratified groups of (**C**) patients. The topographical maps from the large cohort can be used in a user-friendly fashion to grade WMH in patients at risk for stroke. This might have value in both clinical and research settings for the following reasons: (1) current WMH grading systems are subjective and not finely graded (typical scales are mild, moderate, or severe), whereas the new grading system is both objective and finely calibrated, with a solid statistical underpinning for its findings. (2) The grading system is easy to apply in clinic. Each patient’s fluid-attenuation-inversion-recovery MR lesions can simply be visually matched to the grading scales we have provided to generate a percentile rank (please also see Movie in the online-only Data Supplement). (3) The visual nature of the grading system lends itself to patient education and might help clinicians to motivate patients in executing lifestyle changes.

volume in this study corresponds to 7.3 cm³ (interquartile range, 3.5–15.3 cm³), which is similar to the values of prior reports on patients with stroke.^{9,19} However, general population studies have reported relatively small WMH volumes. (Table VI in the online-only Data Supplement).¹⁹

Our patients were either studied as an undivided group or were stratified by hypertension and age as 2 major risk factors. Multivariable analysis on the entire patient population showed that age, hypertension, and LVH were positive predictors of log WMHv, while atrial fibrillation was a negative predictor, independent of other factors including sex, prior use of antiplatelets, and smoking. log WMHv was estimated to increase by 0.38 (≈1.46% of brain volume) per 10 years of aging and by 0.21 (≈1.23% of brain volume) in the presence of hypertension.

log WMHv increased linearly as a function of increasing age. It was notable that patients of similar age had variable WMH volumes (Figure V in the online-only Data Supplement). Considering that age and hypertension are the 2 strongest risk predictors of WMH volume, we stratified our patients by age (≤69 versus ≥70) and the presence or absence of hypertension. In each of the 4 subgroups formed by this stratification, age was consistently associated with increased log WMHv. Topographical frequency-volume maps, multivariable analyses, and statistical parametric mapping also showed that WMH volume was primarily affected by age and secondarily by hypertension.

In the older age groups, the WMH difference between the hypertensive and nonhypertensive patients were only marginally significant. In the younger age groups, however, compared

Table 2. Bivariate and Multivariable Analyses to Identify Risk Factors Associated With White Matter Hyperintensities

Variables	Bivariate*			Multivariable†		
	Yes	No	P Value	Coefficient (SE)	Standardized Coefficient	P Value
Sex, men	0.54 (0.28–1.14)	0.75 (0.36–1.58)	<0.01	0.035 (0.045)	0.017	0.44
Hypertension	0.72 (0.37–1.48)	0.44 (0.20–0.94)	<0.01	0.185 (0.041)	0.089	<0.01
Diabetes	0.62 (0.33–1.30)	0.61 (0.29–1.35)	0.37	0.054 (0.050)	0.027	0.28
Hyperlipidemia	0.60 (0.31–1.23)	0.63 (0.30–1.38)	0.19	−0.043 (0.040)	−0.022	0.28
Smoking, current or quit <5 y	0.51 (0.26–1.06)	0.71 (0.34–1.50)	<0.01	−0.042 (0.044)	−0.021	0.34
Atrial fibrillation	0.67 (0.36–1.25)	0.59 (0.29–1.32)	0.055	−0.179 (0.049)	−0.072	<0.01
Coronary artery disease	0.67 (0.38–1.38)	0.60 (0.29–1.31)	0.09	−0.082 (0.059)	−0.027	0.16
Left ventricular hypertrophy	0.72 (0.37–1.53)	0.60 (0.29–1.29)	<0.01	0.160 (0.055)	0.055	<0.01
Prior use of antiplatelet	0.71 (0.37–1.53)	0.58 (0.29–1.28)	<0.01	0.008 (0.048)	0.003	0.87
Age, y	$\rho=0.501$		<0.01	0.038 (0.002)	0.500	<0.01
Body mass index, kg/m ²	$\rho=-0.091$		<0.01	0.002 (0.006)	0.007	0.73
Total cholesterol, mmol/L	$\rho=-0.040$		0.04	0.022 (0.020)	0.025	0.25
HDL cholesterol, mmol/L	$\rho=-0.005$		0.79	−0.024 (0.062)	−0.008	0.70
LDL cholesterol, mmol/L	$\rho=-0.031$		0.12	Not applicable‡		
HbA1c, %	$\rho=0.014$		0.51	−0.029 (0.016)	−0.043	0.08

HbA1c indicates hemoglobin A1c; HDL, high-density lipoprotein; and LDL, low-density lipoprotein.

*Data were presented median (interquartile range) or Spearman rank correlation coefficient.

†White matter hyperintensity volumes were transformed to a logarithmic scale. Adjusted R^2 was 0.269.

‡LDL cholesterol was not entered into the multivariable model because of multicollinearity.

with the nonhypertensive patients, patients with hypertension had a significantly higher WMH. In addition, older nonhypertensive patients had a significantly higher WMH than younger hypertensive patients. Statistical parametric mapping showed that the hypertension-related increase in the WMHs in younger patients was observed mostly in the posterior half of the centrum semiovale and around the posterior horn of the lateral ventricle, compared with the anterior regions. In contrast, the hypertension-related aggravation of the WMH increase in the older versus younger patients was observed mainly in the anterior half of the brain subcortically. Intriguingly, the literature has consistently shown that the anterior regions of brain exhibit stronger age-related differences than the posterior regions.^{20–22}

In the younger patients with hypertension, but not in the older patients with hypertension, LVH were independently related to \log_{10} WMHv. A few previous studies also reported that the duration and control status of hypertension were associated with WMH independently of hypertension^{23,24} and that subclinical left ventricular dysfunction is associated with WMH.²⁵ Part of the Perindopril Protection Against Recurrent Stroke Study suggested that an active blood pressure-lowering regimen prevented or delayed the progression of WMHs in patients with cerebrovascular disease.²⁶ These data indicate that WMH is another type of target organ damage because of hypertension and could serve as a surrogate marker of blood pressure control in cerebrovascular patients under the age 70. In the older patients with hypertension, however, the variability of \log_{10} WMHv could not be explained by LVH. It is suggested that hypertensive insult may have a ceiling effect on the progression of WMH. Alternatively, many people with severe WMH because of long-standing uncontrolled hypertension might not survive or live stroke-free until their 70s.

In the older patients with hypertension, cholesterol level was a positive predictor of \log_{10} WMHv, but hyperlipidemia was a negative predictor, independent of age and other risk factors. These findings are in line with the results of a previous study on 2 different ischemic stroke cohorts, which also reported that hyperlipidemia was associated with less severe WMHs albeit not adjusted for statin treatment.⁹ Although speculative, cholesterol plays a crucial role in the development and maintenance of synaptic connections and neuronal plasticity and might have exerted protective effects against ischemic damage in the white matter²⁷ that is rich in myelin, of which cholesterol is a major component.

Alternatively, prior statin treatment, which was the most frequently found in the older patients with hypertension, might have attenuated endothelial dysfunction that could contribute to the development of WMHs.²⁸ The relatively frequent use of statin may also explain the positive association between cholesterol level and \log_{10} WMHv in these patients. The associations of \log_{10} WMHv with hyperlipidemia and cholesterol level lost significance after an additional adjustment for statin use. In addition, statin use itself was negatively associated with \log_{10} WMHv in the older nonhypertensive patients. These results are in accordance with a prior report showing that hyperlipidemia and statin use mutually mitigate the susceptibility of brain to ischemic insult.²⁹

Surprisingly, we found an inverse relationship between atrial fibrillation and \log_{10} WMHv in the older patients with hypertension. This finding is in line with a study on Spanish patients with ischemic stroke⁹; however, it contradicts a report from the population-based Rotterdam Scan Study, in which atrial fibrillation was positively associated with WMH.⁷ Atrial fibrillation can cause ischemic stroke in the absence of other risk factors that could increase the volume of WMH. In

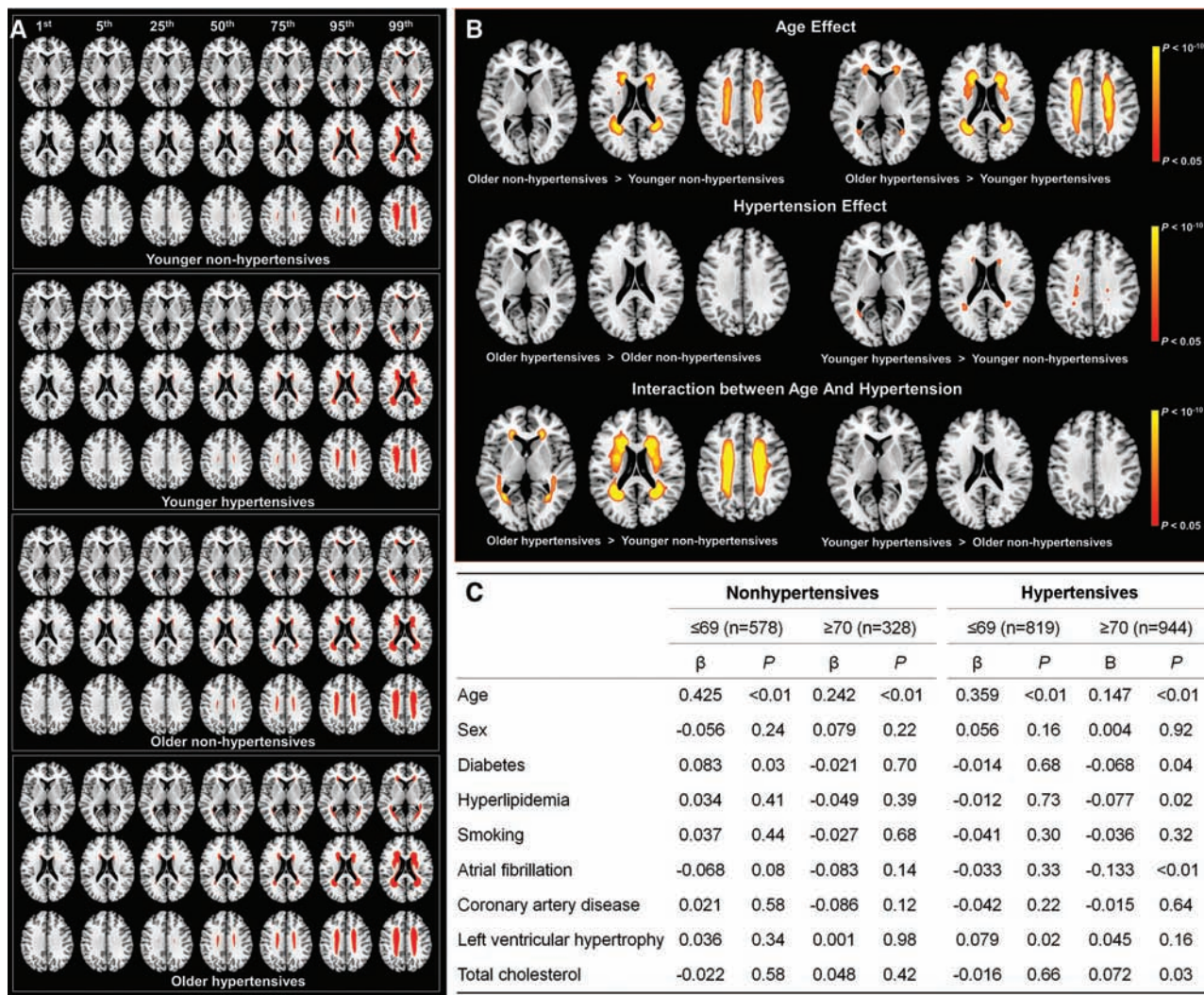


Figure 3. Age/hypertension-adjusted white matter hyperintensity (WMH) maps and vascular risk factors. **A**, In 2669 consecutive patients with first-ever ischemic stroke stratified by the presence of hypertension and age (≤69 vs ≥70), 256 color-coded frequency maps and red color-overlaid frequency-volume maps for WMHs are displayed at 3 representative brain template slices (5.5 mm, 20.5 mm, and 35 mm in z axis of Montreal Neurological Institute space, referred to as the Striatocapsular, Corona Radiata, and Centrum Semiovale levels, respectively). Please note that the total voxel count in the red color-overlaid areas of a frequency-volume map is equal or close to the designated (1%–99%) percentile value of WMH voxel counts in each group of patients. **B**, Statistical parametric mapping visualizes age/hypertension-related effects on WMH volume and distribution: age has a major effect on WMH (**top**), whereas hypertension has only minor effects (**middle**), but there is an interactive effect of both together (**bottom**). Based on 2-dimensional random field theory,^{20,21} statistical parametric mapping analyses are performed to produce corrected P value maps comparing the regional differences in the frequency of having WMH (at each voxel) between age- and hypertension-stratified groups. For a more detailed interpretation of these statistical parametric mapping results, please see the Results in the online-only Data Supplement. **C**, Multiple regression analyses (β=standardized coefficient) after the stratification by age (≤69 vs ≥70) and hypertension identify subgroup-specific predictors of WMH volume. WMH volumes were transformed to a logarithmic scale by using the equation log (WMH volume+0.05) after considering that the frequency distribution of WMH volumes was skewed and some patients had no WMH. By taking into account both age/hypertension-adjusted topographical frequency-volume maps and age/hypertension-adjusted multivariable analysis results, one may pose that a younger patient with a high rank percentile of WMH has an undiagnosed condition, such as diabetes mellitus or left ventricular hypertrophy, and then go looking for these diseases. Contrariwise, if an elderly patient despite having hypertension ranks low (ie, low WMH burden), we might pose that WMH-related risk factors may have been well controlled or that there might be an unknown (eg, genetically) protective effect for preventing white matter lesions.

general population, however, a positive association between atrial fibrillation and WMH volume is likely to be observed, because hypertension, which acts to increase the volume of WMH, is a major risk factor for atrial fibrillation.³⁰

Several lines of evidence have suggested a positive relationship between diabetes mellitus and WMH, albeit not consistently.^{8,31,32} One study reported that diabetes mellitus was related to WMH in younger patients (<75 years) but not in the

elderly.³¹ Of note, the frequency of hypertension in the study was as low as 26%.³¹ In addition, another study, in which the mean age was as low as 54.7 years and hypertension was not associated with WMH, also demonstrated an independent association between diabetes mellitus and WMH.³² However, other studies that included elderly and hypertensive subjects have rarely showed significant relationships between diabetes mellitus and WMH.^{33,34} Likewise, in our study, diabetes

mellitus was an independent negative predictor of \log_{10} WMHv in the older patients with hypertension. In contrast, diabetes mellitus was a positive independent predictor in the younger nonhypertensive patients. Thus, diabetes mellitus does seem to contribute to the WMH pathology while possibly increasing the frequency and severity of hypertensive vascular events. Subsequently, an increase of cardiovascular mortality or earlier stroke onset before the age 70 might reduce the incidence of first-ever stroke in hypertensive diabetic patients after the age 70, who would have extensive WMH.

When we split our patient population by stroke pathogenesis into SVO and non-SVO subgroups, the presence of hypertension could explain more of the data variability in the SVO subgroup than in the non-SVO subgroup, after adjustment for other WMH risk factor covariates. This implies that hypertension had a differential impact in the SVO group, being associated with higher WMH-increasing effects than in the non-SVO group. The effects of aging did not show this differential, and showed similar standardized coefficients both in the SVO and non-SVO subgroups. These findings suggest a higher vulnerability of SVO (as opposed to non-SVO) patients to hypertension-mediated white matter injury (please see Discussion in the online-only Data Supplement). In addition, SVO stroke was associated with a larger age-adjusted WMH volume compared with other stroke subtypes, which is in line with a previous report.³⁵

Because of the multiplicity of data, hypotheses, and analyses,³⁶ results of this descriptive study need careful interpretation, as well as further confirmatory research. First, the statistical map-based visual volume assessment method that we provide could yield an equal WMH percentile rank for contiguous or multiple scattered lesions (as long as the total volume is equal) in a clinical setting. Second, our study population is from a single ethnicity, at presentation with a first-ever ischemic stroke, which may limit the applicability of our data to more general populations with varying ethnicities and disease profiles. We focused on patients with first-ever stroke, whose WMH were not attributable to clinically evident prior stroke. In addition, we have made great efforts to enroll the subjects in a consecutive manner to minimize any selection bias that may have caused inconsistent associations between various risk factors and WMH in prior studies. Furthermore, WMH-related factors that were found in this study were largely, although not wholly (Table VII in the online-only Data Supplement), comparable to those of previous studies on general elderly or high-risk populations.^{25,37} However, future studies must confirm that the current results from our first-ever stroke patient population could also be extrapolated to high-risk patients who have not yet had stroke. Third, a correlative study cannot aspire to establish causality, and our study, using a cross-sectional design is certainly not suited to establish a causal link between WMH and, for example, subsequent risk of stroke. But, it does allow causal hypotheses to be posed (Figure 3) and tested in a more quantifiable manner. We hope that our reference data will help to pose interesting hypotheses and provide tools to execute future studies aimed at establishing causal relationships.

Conclusions

This is the first, large nationwide multicenter study to report on the incidence and volume of WMH in patients with first-time stroke. We find age and hypertension to be the strongest predictors of WMH. We derived visual reference data sets, including age and hypertension-adjusted statistical frequency-volume maps to allow the easy statistical ranking of WMH in individual clinic patients. Our data, based on a large population, and rigorously analyzed with topographical statistical analysis, could serve as a useful grading system for WMH and as a tool to further trials and studies.

Acknowledgments

We thank Eun Kyoung Hwang, Sun-young Chung, Yu-Hwa Kim, Jung Ok Nam, Eun-Hee Park, Min-Kyung Yang, and Hyo Eun Jeon for their assistance with this research. We are grateful to all medical staff, staff nurses, and research nurses at the 11 sites, who contributed greatly to the successful conduct of the study.

Sources of Funding

This study was supported by grants (to Dong-Eog Kim) from National Center for Standard Reference Data, Ministry of Trade, Industry & Energy and Ministry of Health & Welfare (A121996; Korea Healthcare Technology R&D Project), Republic of Korea.

Disclosures

None.

References

- Hajjar I, Quach L, Yang F, Chaves PH, Newman AB, Mukamal K, et al. Hypertension, white matter hyperintensities, and concurrent impairments in mobility, cognition, and mood: the Cardiovascular Health Study. *Circulation*. 2011;123:858–865.
- Wardlaw JM, Smith C, Dichgans M. Mechanisms of sporadic cerebral small vessel disease: insights from neuroimaging. *Lancet Neurol*. 2013;12:483–497.
- Debette S, Markus HS. The clinical importance of white matter hyperintensities on brain magnetic resonance imaging: systematic review and meta-analysis. *BMJ*. 2010;341:c3666.
- Lee SH, Kim BJ, Ryu WS, Kim CK, Kim N, Park BJ, et al. White matter lesions and poor outcome after intracerebral hemorrhage: a Nationwide Cohort Study. *Neurology*. 2010;74:1502–1510.
- Godin O, Tzourio C, Maillard P, Mazoyer B, Dufouil C. Antihypertensive treatment and change in blood pressure are associated with the progression of white matter lesion volumes: the Three-City (3C)-Dijon Magnetic Resonance Imaging Study. *Circulation*. 2011;123:266–273.
- Basile AM, Pantoni L, Pracucci G, Asplund K, Chabriat H, Erkinjuntti T, et al; LADIS Study Group. Age, hypertension, and lacunar stroke are the major determinants of the severity of age-related white matter changes. The LADIS (Leukoaraiosis and Disability in the Elderly) Study. *Cerebrovasc Dis*. 2006;21:315–322.
- de Leeuw FE, de Groot JC, Oudkerk M, Kors JA, Hofman A, van Gijn J, et al. Atrial fibrillation and the risk of cerebral white matter lesions. *Neurology*. 2000;54:1795–1801.
- Jeerakathil T, Wolf PA, Beiser A, Massaro J, Seshadri S, D'Agostino RB, et al. Stroke risk profile predicts white matter hyperintensity volume: the Framingham Study. *Stroke*. 2004;35:1857–1861.
- Jimenez-Conde J, Biffi A, Rahman R, Kanakis A, Butler C, Sonni S, et al. Hyperlipidemia and reduced white matter hyperintensity volume in patients with ischemic stroke. *Stroke*. 2010;41:437–442.
- Smith EE. Leukoaraiosis and stroke. *Stroke*. 2010;41:S139–S143.
- Carmelli D, DeCarli C, Swan GE, Jack LM, Reed T, Wolf PA, et al. Evidence for genetic variance in white matter hyperintensity volume in normal elderly male twins. *Stroke*. 1998;29:1177–1181.
- Atwood LD, Wolf PA, Heard-Costa NL, Massaro JM, Beiser A, D'Agostino RB, et al. Genetic variation in white matter hyperintensity volume in the Framingham Study. *Stroke*. 2004;35:1609–1613.

13. Kim BJ, Han MK, Park TH, Park SS, Lee KB, Lee BC, et al; CRCS-5 investigators. Current status of acute stroke management in Korea: a report on a multicenter, comprehensive acute stroke registry. *Int J Stroke*. 2014;9:514–518.
14. Kim DE, Park KJ, Schellingerhout D, Jeong SW, Ji MG, Choi WJ, et al. A new image-based stroke registry containing quantitative magnetic resonance imaging data. *Cerebrovasc Dis*. 2011;32:567–576.
15. Lim JS, Kim N, Jang MU, Han MK, Kim S, Baek MJ, et al. Cortical hubs and subcortical cholinergic pathways as neural substrates of poststroke dementia. *Stroke*. 2014;45:1069–1076.
16. Kim DE, Kim JY, Schellingerhout D, Kim EJ, Kim HK, Lee S, et al. Protease imaging of human atheromata captures molecular information of atherosclerosis, complementing anatomic imaging. *Arterioscler Thromb Vasc Biol*. 2010;30:449–456.
17. Kim DE, Kim JY, Nahrendorf M, Lee SK, Ryu JH, Kim K, et al. Direct thrombus imaging as a means to control the variability of mouse embolic infarct models: the role of optical molecular imaging. *Stroke*. 2011;42:3566–3573.
18. Kwon JY, Rhyu IJ, Cheon JJ, Koh IS. Brain volume measurement of healthy Korean for clinical application using MRI. *The Report of National Institute of Health*. 2001;38:279–284.
19. Schwartz GL, Bailey KR, Mosley T, Knopman DS, Jack CR Jr, Canzanello VJ, et al. Association of ambulatory blood pressure with ischemic brain injury. *Hypertension*. 2007;49:1228–1234.
20. Head D, Buckner RL, Shimony JS, Williams LE, Akbudak E, Conturo TE, et al. Differential vulnerability of anterior white matter in nondemented aging with minimal acceleration in dementia of the Alzheimer type: evidence from diffusion tensor imaging. *Cereb Cortex*. 2004;14:410–423.
21. Ardekani S, Kumar A, Bartzokis G, Sinha U. Exploratory voxel-based analysis of diffusion indices and hemispheric asymmetry in normal aging. *Magn Reson Imaging*. 2007;25:154–167.
22. Abe O, Aoki S, Hayashi N, Yamada H, Kunimatsu A, Mori H, et al. Normal aging in the central nervous system: quantitative MR diffusion-tensor analysis. *Neurobiol Aging*. 2002;23:433–441.
23. van Dijk EJ, Breteler MM, Schmidt R, Berger K, Nilsson LG, Oudkerk M, et al; CASCADE Consortium. The association between blood pressure, hypertension, and cerebral white matter lesions: cardiovascular determinants of dementia study. *Hypertension*. 2004;44:625–630.
24. de Leeuw FE, de Groot JC, Oudkerk M, Witteman JC, Hofman A, Gijn J, et al. Hypertension and cerebral white matter lesions in a prospective cohort study. *Brain*. 2002;125(pt 4):765–772.
25. Russo C, Jin Z, Homma S, Elkind MS, Rundek T, Yoshita M, et al. Subclinical left ventricular dysfunction and silent cerebrovascular disease: the Cardiovascular Abnormalities and Brain Lesions (CABL) study. *Circulation*. 2013;128:1105–1111.
26. Dufouil C, Chalmers J, Coskun O, Besançon V, Bousser MG, Guillon P, et al; PROGRESS MRI Substudy Investigators. Effects of blood pressure lowering on cerebral white matter hyperintensities in patients with stroke: the PROGRESS (Perindopril Protection Against Recurrent Stroke Study) Magnetic Resonance Imaging Substudy. *Circulation*. 2005;112:1644–1650.
27. Mauch DH, Nägler K, Schumacher S, Göritz C, Müller EC, Otto A, et al. CNS synaptogenesis promoted by glia-derived cholesterol. *Science*. 2001;294:1354–1357.
28. Mason RP, Walter MF, Jacob RF. Effects of HMG-CoA reductase inhibitors on endothelial function: role of microdomains and oxidative stress. *Circulation*. 2004;109:II34–II41.
29. Rost NS, Fitzpatrick K, Biffi A, Kanakis A, Devan W, Anderson CD, et al. White matter hyperintensity burden and susceptibility to cerebral ischemia. *Stroke*. 2010;41:2807–2811.
30. Benjamin EJ, Levy D, Vaziri SM, D'Agostino RB, Belanger AJ, Wolf PA. Independent risk factors for atrial fibrillation in a population-based cohort. The Framingham Heart Study. *JAMA*. 1994;271:840–844.
31. Ylikoski A, Erkinjuntti T, Raininko R, Sarna S, Sulkava R, Tilvis R. White matter hyperintensities on MRI in the neurologically nondiseased elderly. Analysis of cohorts of consecutive subjects aged 55 to 85 years living at home. *Stroke*. 1995;26:1171–1177.
32. Schmidt R, Fazekas F, Kleinert G, Offenbacher H, Gindl K, Payer F, et al. Magnetic resonance imaging signal hyperintensities in the deep and subcortical white matter. A comparative study between stroke patients and normal volunteers. *Arch Neurol*. 1992;49:825–827.
33. Breteler MM, van Swieten JC, Bots ML, Grobbee DE, Claus JJ, van den Hout JH, et al. Cerebral white matter lesions, vascular risk factors, and cognitive function in a population-based study: the Rotterdam Study. *Neurology*. 1994;44:1246–1252.
34. Webb AJ, Simoni M, Mazzucco S, Kuker W, Schulz U, Rothwell PM. Increased cerebral arterial pulsatility in patients with leukoaraiosis: arterial stiffness enhances transmission of aortic pulsatility. *Stroke*. 2012;43:2631–2636.
35. Rost NS, Rahman RM, Biffi A, Smith EE, Kanakis A, Fitzpatrick K, et al. White matter hyperintensity volume is increased in small vessel stroke subtypes. *Neurology*. 2010;75:1670–1677.
36. Bender R, Lange S. Adjusting for multiple testing—when and how? *J Clin Epidemiol*. 2001;54:343–349.
37. Rostrup E, Gouw AA, Vrenken H, van Straaten EC, Ropele S, Pantoni L, et al; LADIS Study Group. The spatial distribution of age-related white matter changes as a function of vascular risk factors—results from the LADIS study. *Neuroimage*. 2012;60:1597–1607.

SUPPLEMENTAL MATERIAL

Grading and Interpretation of White Matter Hyperintensities Using Statistical Maps

Online Supplemental Contents

Supplemental Methods

Supplemental Results

Supplemental Discussion

Supplemental Table I. Summary of literature on the association between risk factors and white matter hyperintensities

Supplemental Table II. Imaging protocols of participating centers

Supplemental Table III. Fluid-attenuated inversion recovery (FLAIR) parameters and number of patients

Supplemental Table IV. Multivariable association of vascular risk factors with WMH volume in patients with acute ischemic stroke due to small vessel occlusion (SVO) vs. other etiologies (non-SVO)

Supplemental Table V. Multivariable relationship between risk factors and white matter hyperintensities volume after stratification by hypertension and age (≤ 69 years and ≥ 70 years): further adjustment for prior statin use

Supplemental Table VI. Literature review on white matter hyperintensity volume: comparison with the present study

Supplemental Table VII. A modified version of the Supplemental Table I, with the literature summary reorganized based on the mean age and prevalence of hypertension, for comparison with the present study

Supplemental Table VIII. Patient characteristics: comparison between two different magnetic field strengths (1.5 Tesla vs. 3.0 Tesla)

Supplemental Figure I. Distribution of participating centers and enrollment of study subjects and study flow chart

Supplemental Figure II. Registration of white matter hyperintensity lesions on the template using a custom-built software package

Supplemental Figure III. Estimation of white matter hyperintensity volume percentages while adjusting for the effects of different spacing of source MRIs and template images

Supplemental Figure IV. Correlation between white matter hyperintensity (WMH) volume calculations in the template image space (used for the lesion registration and quantification for the main studies) and WMH volume calculations done in the original FLAIR MRI space

Supplemental Figure V. Scatter plots and linear regressions (equations and R-square on figures) to show the age / hypertension-dependence of white matter hyperintensity volume

Supplemental Figure VI. Age-adjusted white matter hyperintensity volumes in different stroke subtypes

Supplemental Figure VII. t-values for interaction between hypertension and dichotomized age

Supplemental Figure VIII. Box plots with scatter plots for white matter hyperintensities:

comparison between two different magnetic field strengths (1.5T vs. 3T)

Supplemental Figure IX. Inter-rater reliability of the measurement of white matter hyperintensity volume

Supplemental Video. Examples of using the new visual grading system for white matter hyperintensity

Supplemental References

Supplemental Methods

Vascular risk factors

Hypertension was defined as systolic blood pressure ≥ 140 mm Hg after stabilization of neurological and medical condition or pre-stroke treatment with antihypertensive drugs.¹ Diabetes was defined as previous diagnosis of type I or II diabetes, fasting blood glucose ≥ 7.0 mmol/l (126 mg/dl) or HbA1c $\geq 6.5\%$, or a history of taking hypoglycemic agents.² Hyperlipidemia was defined as a fasting serum cholesterol level ≥ 6.2 mmol/l (240 mg/dl), a fasting low-density lipoprotein level ≥ 4.1 mmol/l (160 mg/dl), or previous diagnosis of hyperlipidemia with current use of lipid-lowering medications.³ Coronary artery disease was defined as a history of myocardial infarction, angina, percutaneous coronary intervention, or coronary bypass surgery. Left ventricular hypertrophy (LVH) was diagnosed by using electrocardiogram or echocardiogram. Smokers were defined as patients who reported current smoking or quit smoking ≤ 5 years. Initial neurologic severity was estimated using the National Institutes of Health Stroke Scale. Subtypes of index stroke were determined by the consensus of experienced neurologists of each participating centers as follows; large artery disease, small vessel occlusion, cardioembolism, other determined etiology, and undetermined etiology, as described in Trial of Org 10172 in Acute Stroke Treatment (TOAST).⁴

Brain MRI and quantitative image registration

Brain MRI was performed on 1.5-Tesla ($n = 2,338$) or 3.0-Tesla ($n = 331$) MRI system (Table II in the online-only Data Supplement). Fluid-attenuated inversion recovery (FLAIR) protocols were TE 76–160ms, TR 6000–11,000ms, voxel size $1 \times 1 \times 3 \sim 1 \times 1 \times 7 \text{ mm}^3$, interslice gap 0–2.25mm, FOV 250mm, and matrix size 256×256 . All scans were transferred to the Korean Brain MRI Data Center for central data storage and quantitative image analysis. As previously reported,^{5, 6} in every patient all FLAIR MRIs were converted into a patient-independent quantitative visual format. Brain template images were prepared (139 slices, $0.5 \times 0.5 \times 1 \text{ mm}^3$ voxels) from the Montreal Neurological Institute (MNI) ch2better-template (316 slices, $0.5 \times 0.5 \times 0.5 \text{ mm}^3$ voxels) within the range of -63.5 to 74.5 mm in the Z-axis of Talairach space. After normalization of images, each patient's high signal intensity lesions on FLAIR MRIs were semi-automatically segmented and registered onto the brain templates (Figure II in the online-only Data Supplement) under close supervision by vascular neurologists. To do this, the assistants did the following: a) segment white matter hyperintensity (WMH) by manually drawing a region of interest (ROI) containing high signal intensity lesions and clicking on any WMH-related pixel inside the ROI, providing a starting point for the smart region selection algorithm of Image_QNA to select the lesions to the first approximation, b) adjust the initial segmentation by the exclusion or inclusion of additional pixels of similar signal intensity range by rolling the wheel of the computer mouse up or down, c) exclude fresh stroke related signal, based on a careful comparison between FLAIR and diffusion-weighted images, by using image-editing tools of the software package, d) find the corresponding template image, e) let the software automatically transfer the selected lesions to the template while distorting the x and y scales of the image/template, f) make fine adjustments to the location, size, and shape of the lesions by using the image-editing tools, and g) save the final data.

As described above, only chronic WMH lesions were registered by excluding the FLAIR high signal lesions due to acute infarction.⁷ When chronic lesions on FLAIR and acute lesions on diffusion-weighted image overlapped, the extent and distribution of FLAIR WMH contralateral to the location of acute infarct served as a reference to determine what volumes to include and exclude, by assuming a symmetric distribution of WMH across the midline. This semiautomatic method was shown to produce more accurate results than the statistical parametric mapping (SPM)-based automatic method.⁵ During the process of quantification for WMH lesion volume, the inter-rater variability was minimal (Figure VIII in the online-only Data Supplement). Furthermore, intra-observer correlation coefficient was also high, ranging from 0.987 to 0.995 (data not shown).

WMH volume was calculated as a simple percentage of the number of voxels included in registered

lesions (in the template space) divided by the total number of brain parenchymal voxels (in the template space), with both the numerator and denominator adjusted for differences in slice spacing (i.e. slice thickness and interslice gap) between acquisition (FLAIR MR) images and template images (Table III and Figure III in the online-only Data Supplement). We validated our method of WMH volume (%) measurement in 163 randomly selected patients from Dongguk University Ilsan Hospital. In these patients, in addition to the template based approach described above, we also did WMH voxel counts and brain parenchymal voxel counts in the native MR space using the raw images in each patient. We calculated the total number of voxels in WMH lesions, which was then divided by the total number of voxels in the whole brain parenchyma, and then multiplied by 100.⁸ These template based and raw image based WMH percentages were correlated to provide verification of our volumetric methodology.

WMH Frequency-Volume Maps

For WMH lesion mapping, we used three MNI template slices (centered on 5.5mm, 20.5mm, and 35mm on the Z-axis) that represent the levels of striatocapsular ($5.5 \pm 5\text{mm}$), corona radiata ($20.5 \pm 5\text{mm}$), and centum semiovale ($35 \pm 5\text{mm}$) regions, respectively. In each of these three slices, a WMH frequency map was constructed as previously published^{5, 9, 10} by plotting the frequency of incidence of WMH lesions at each voxel coordinate of the slice as a heat map (Figure 1 in the main manuscript). At each level, the number of voxels involved in all patients or a group of patients are listed in rank order, and assigned a percentile value based on their position in the list. Then, voxels in the color-coded area of a frequency map were collected in the order of their RGB values [(255, 0, 0) \rightarrow (0, 255, 0) \rightarrow (0, 0, 255)] until the total voxel count reached the number closest to a chosen number that corresponded to a percentile value of WMH voxel counts (at each level) in all patients or a group of patients. Then, to facilitate the use of our data as reference standard for grading purposes of WMH, we plotted the data as frequency-volume maps to show the statistical volume and spatial distribution in a single format, arranged to reflect the percentile distribution of disease in our study population (Figure 1 in the main manuscript).

Statistical analyses

Data are presented as mean \pm standard deviation, median (interquartile range) or number (percentage), as appropriate. Inter-group differences and bivariate associations of WMH volume were assessed using nonparametric tests (Kruskal-Wallis test, Mann-Whitney *U*-test, or Spearman correlation) because of a skewed distribution of WMHs. Multiple linear regression analysis was performed to identify independent risk factors of WMH volume. For this analysis, as a dependent variable we used (natural) log-transformed WMH volume ($\log \text{WMHv}$): $\log(\text{WMH volume} + 0.05)$ due to skewed distribution of WMHs and some patients having no WMH. The normality of $\log \text{WMHv}$ was evaluated using the Kolmogorov-Smirnov test. In the multiple regression model, predefined variables reportedly associated with WMH in previous studies were used as independent variables.¹¹⁻¹⁴ We further adjusted for the prior use of statins to investigate an independent association of hyperlipidemia or cholesterol levels with $\log \text{WMHv}$.

Small vessel occlusion (SVO), as compared to other stroke subtypes, is known to have a closer association with WMH.¹⁵ Thus, in order to compare WMH volumes between stroke subtypes, age-adjusted $\log \text{WMHv}$ was calculated by using marginal linear prediction after ANOVA, followed by pairwise comparison with a Bonferroni correction.¹⁶ In addition, multiple linear regression analysis was performed to evaluate the associations between WMH volume and risk factors in patients with SVO stroke (n=454) vs. non-SVO stroke (n=2126; large artery disease, cardioembolism, and undetermined subtypes pooled together as one group).

Age and hypertension are the most consistent and strong risk factors for WMHs.¹⁷ Thus, to refine our statistical analyses and allow lesion maps to be tailored more precisely, the patients were stratified by the presence of hypertension and/or age. Dichotomization of age was done at 69 years (≤ 69 vs. ≥ 70) because the median age of our patients was 69. In addition, a previous study that investigated interactive effects of age and

hypertension on volumes of brain structure while adjusting for WMH severity divided their subjects by age of 69 years.¹⁸ Post-hoc analysis showed that the largest interaction effect between hypertension and age on \log_{10} WMHv was observed when ages were dichotomized at 69 years (t for interaction = -3.65, $P < 0.01$, Figure IX in the online-only Data Supplement).

Multiple linear regression analyses were performed independently for each of the four groups formed by the age-hypertension matrix. Thereafter, based on 2D random field theory,^{19, 20} statistical parametric mapping analyses were performed using a custom-written program to produce corrected P -value maps comparing the regional differences in the frequency of having WMH (at each voxel) between age and hypertension-stratified groups. All the analyses were performed using the R package, STATA 13.0 (Stata-Corp, College Station, TX) and MATLAB (MathWorks Inc., Natick, MA). $P < 0.05$ was considered statistically significant.

Supplemental Results

There was a strong linear correlation (R-square = 0.86, $P < 0.01$) between volume calculations in the original source MR image space and the volume calculations that were done in the template space and used for the main studies (Figure IV in the online-only Data Supplement), indicating that our template based approach is valid, and a close approximation of raw volume calculations.

Multivariable analysis showed that in the SVO subgroup, compared with the non-SVO subgroup, the presence of hypertension had a higher standardized coefficient (Table IV in the online-only Data Supplement). In addition to the presence of hypertension, LVH was a statistically significant independent predictor of WMH volume in the non-SVO subgroup ($P < 0.01$), whereas the association was only marginally significant in the SVO subgroup ($P = 0.06$). It is also notable that male sex was significantly associated with WMH in the SVO subgroup, but not in the non-SVO subgroup.

Statistical parametric mapping to show the age and hypertension-related effects on WMH

P -value maps of the non-hypertensive patients (older non-hypertensives > younger non-hypertensives) corrected for multiple comparisons revealed regions of significantly higher WMH frequency in the older vs. younger patients (Upper panel of Figure 3B in the main manuscript). The significant clusters were observed in the centrum semiovale at the Centrum Semiovale level and around the anterior and posterior horns of the lateral ventricle at the Corona Radiata level.

Compared with the non-hypertensive patients, in the P -value maps of the hypertensive patients (older hypertensives > younger hypertensives) corrected for multiple comparisons, there were relatively extensive regions with significantly higher WMH frequency in the older vs. younger patients (Figure 3B in the main manuscript). The hypertension-related increase in the extents of regions with significantly higher WMH frequency in the older vs. younger patients were mainly observed in the anterior half of the centrum semiovale at the Centrum Semiovale level and around the anterior horns of the lateral ventricle at the Corona Radiata and Striatocapsular level, compared with the posterior portions.

In the P -value maps of younger patients (younger hypertensives > younger non-hypertensives) corrected for multiple comparisons, there were limited regions with significantly higher WMH frequency in the hypertensive vs. non-hypertensive patients (Middle panel of Figure 3B in the main manuscript). The extent of the significant clusters was larger around the posterior horns and posterior half of the centrum semiovale, compared with anterior portions. In the P -value maps of the older patients (older hypertensives > older non-hypertensives), significant clusters were barely observed.

The extent of regions with significantly higher WMH frequency was largest for older hypertensive vs. younger non-hypertensive patients, followed by older non-hypertensive vs. younger hypertensive patients (Lower panel of Figure 3B in the main manuscript). ANOVA and post-hoc analyses with Bonferroni correction supported these findings (all $P < 0.01$) except between the latter two groups showing a marginal significant difference ($P = 0.08$). There was no region with significantly higher WMH frequency either for younger non-hypertensive vs. older hypertensive patients or younger hypertensive vs. older non-hypertensive patients.

Supplemental Discussion

We performed a subgroup analysis in patients with stroke due to SVO vs. non-SVO, and found suggestions that hypertension had a differentially higher impact in the SVO group. There were higher WMH volumes associated with hypertension in the SVO group, than in the non-SVO group. When adjusting for the presence of hypertension, we found a stronger than expected relationship between LVH and WMH for non-SVO patients, as opposed to SVO patients. This likely suggests that the duration and control status of hypertension are relatively more important in the WMH pathogenesis of non-SVO patients. In the SVO patients however, it is speculated that the presence of hypertension (by itself) might be strong enough to have an early ceiling effect on the progression of WMH. This seems to be in line with the relatively strong association between WMH volume and the presence of hypertension in the SVO subgroup compared with the non-SVO subgroup. However, these data and speculations should be viewed as hypotheses suggested by our analysis, and would need to be confirmed in future, preferably prospective, studies.

Supplemental Table I. Summary of literature on the association between risk factors and white matter hyperintensities

Year	Author	Population	No. of subjects	Mean age	Prevalence of HT	Measure	Risk factors related to white matter hyperintensities
1986	Awad et al. ²¹	General population with or without stroke	82	64	40%	Grading	Age, prior stroke, hypertension
1992	Schmidt et al. ²²	General population with or without stroke	234	55	35%	Grading	Age, diabetes
1995	Ylikoski et al. ²³	General population without stroke	128	72	28%	Grading	Age
1996	Longstreth et al. ²⁴	General population without stroke	3301	75	45%	Grading	Age, sex, smoking, race, hypertension, cardiovascular disease, LVH
2000	Hirono et al. ²⁵	Demented patients with or without stroke	131	74	30%	Grading	Age, hypertension
2004	Jeerakathil et al. ²⁶	General population without stroke	1814	62	18%	Quantitative	Age, smoking, cardiovascular disease, hypertension, LVH
2007	Khan et al. ²⁷	Ischemic stroke	414	69	89%	Grading	Age, diabetes (inverse), hyperlipidemia (inverse), cardiovascular disease (inverse)
2007	Schwartz et al. ¹⁴	General population without stroke*	610	63	81%	Quantitative	Age, hypertension, homocysteine, sex (only white)
2010	Jimenez-Conde et al. ²⁸	Ischemic stroke [†]	631	65	62%	Quantitative	Age, hyperlipidemia (inverse), smoking
2010	Jimenez-Conde et al. ²⁸	Ischemic stroke [‡]	504	69	67%	Grading	Age, sex, hypertension, hyperlipidemia (inverse), atrial fibrillation (inverse), prior stroke
2010	Rost et al. ²⁹	Ischemic stroke	602	65	62%	Quantitative	Age, atrial fibrillation, cardiovascular disease
2012	Rostrup et al. ³⁰	General population with or without stroke	695	74	70%	Quantitative	Age, hypertension, smoking

HT indicates hypertension; and LVH, left ventricular hypertrophy.

*White (n=343) and black (n=267) US adults

[†]US patients

[‡]Spanish patients

Supplemental Table II. Imaging protocols of participating centers

Hospital	Scanner name, Company	Tesla	Slice Thickness	Slice Spacing	TR(ms)/TE(ms)	No. of patients
	Achieva, Philips	3	5	6	11000/125	182
Hospital A	Intera , Phillips	1.5	5	6	11000/140	161
	Intera , Phillips	1.5	5	6	6000/120	44
Hospital B	Signa Exite Twin Speed, G.E.	1.5	5	6	10000/160	84
	Skyra, Siemens	3	5	6	9000/76	4
	Symphony Vision, Siemens	1.5	5	6	9000/117	91
Hospital C	Sonata, Siemens	1.5	5	6	9000/122	113
	Skyra, Siemens	3	5	6	9000/95	28
Hospital D	Avanto, Siemens	1.5	5	7	8000/93	176
	Signa Exite Twin Speed, G.E.	1.5	5	7	8002/127	179
Hospital E	Signa Exite Twin Speed, G.E.	1.5	5	7	8002/134	85
	Magnetom Vision, Siemens	1.5	5	7	9000 / 117	101
Hospital F	Achieva, Philips	3	5	7	8000/120	62
	Avanto, Siemens	1.5	5	7	8500/112	22
	Sonata, Siemens	1.5	5	6	10000/99	4
Hospital G	Sonata, Siemens	1.5	5	6.25	10000/99	8
	Sonata, Siemens	1.5	5	6.5	10000/99	71
Hospital H	Intera , Phillips	1.5	5	7	9000/140	370
	Avanto, Siemens	1.5	5	6	9000/93	97
Hospital I	Avanto, Siemens	1.5	5	6.5	9000/93	4
	Symphony Tim, Siemens	1.5	5	6	9000/98	72
	Signa HDXT, G.E.	1.5	5	5.5	8802/144	262
Hospital J	Signa HDXT, G.E.	1.5	5	6	8802/144	288
	Signa HDXT, G.E.	1.5	5	6.5	8802/144	3
	Triotim, Siemens	3	5	5.5	7700/88	6
Hospital K	Achieva, Philips	3	5	7	9000/120	44
	Intera , Phillips	1.5	5	7	11000/140	93
Outside film	Variable					45

Supplemental Table III. Fluid-attenuated inversion recovery (FLAIR) MRI parameters and number of patients

Slice Thickness	Slice Spacing	Number of Voxels in Selected Slices of the Template	Number of Patients
3	3	2155881	1
4	5	1289099	1
5	5.3	1289174	8
5	5.5	1078020	262
5	5.75	1078020	1
5	6	1078020	1168
5	6.25	1078020	8
5	6.5	917480	86
5	7	917480	1072
5	7.25	917480	4
5	7.5	806611	4
6	7	917766	48
6	7.2	917766	2
6	7.5	806654	1
6	7.8	806654	1
7	8	806737	1

Supplemental Table IV. Multivariable association of vascular risk factors with WMH volume in patients with acute ischemic stroke due to small vessel occlusion (SVO) vs. other etiologies (non-SVO)

	Non-small vessel occlusion (n = 2126)			Small vessel occlusion (n=454)		
	Coefficient (standard error)	Beta	<i>P</i>	Coefficient (standard error)	Beta	<i>P</i>
Age	0.038 (0.002)	0.488	<0.001	0.038 (0.004)	0.504	<0.001
Sex, men	0.005 (0.050)	-0.004	0.92	0.310 (0.111)	0.162	0.006
Body mass index	0.002 (0.007)	0.010	0.77	-0.013 (0.013)	-0.044	0.34
Hypertension	0.163 (0.047)	0.073	0.001	0.249 (0.087)	0.128	0.004
Diabetes	0.082 (0.056)	0.042	0.14	-0.002 (0.111)	-0.001	0.99
Hyperlipidemia	-0.023 (0.045)	-0.012	0.61	-0.044 (0.092)	-0.023	0.63
Smoking	-0.040 (0.050)	-0.016	0.42	-0.179 (0.108)	-0.096	0.10
Coronary artery disease	-0.085 (0.063)	-0.035	0.18	0.317 (0.195)	0.071	0.11
Prior use of antiplatelet	-0.069 (0.052)	-0.025	0.18	0.202 (0.114)	0.079	0.08
LVH	0.163 (0.061)	0.056	0.008	0.208 (0.118)	0.076	0.08
Total cholesterol	0.037 (0.022)	0.035	0.09	-0.004 (0.049)	-0.004	0.94
HDL cholesterol	-0.040 (0.070)	-0.016	0.57	0.085 (0.152)	0.027	0.57
HbA1c	-0.029 (0.018)	-0.046	0.12	-0.018 (0.035)	-0.029	0.61

Non-SVO infarctions include large artery disease, cardioembolic, and undetermined etiology strokes.

Beta denotes standardized coefficient.

LVH indicates left ventricular hypertrophy.

R-square values were 0.27 and 0.33 for the non-SVO subgroup and SVO subgroup, respectively.

Supplemental Table V. Multivariable relationship between risk factors and white matter hyperintensities volume* after stratification by hypertension and age (≤ 69 years and ≥ 70 years): further adjustment for prior statin use

	Non-hypertensives				Hypertensives			
	≤ 69 (n = 578)		≥ 70 (n = 328)		≤ 69 (n = 819)		≥ 70 (n = 944)	
	Standardized Coefficient	<i>P</i>	Standardized Coefficient	<i>P</i>	Standardized Coefficient	<i>P</i>	Standardized Coefficient	<i>P</i>
Age	0.425	< 0.01	0.239	< 0.01	0.363	< 0.01	0.151	< 0.01
Sex	-0.054	0.27	0.062	0.34	0.054	0.17	-0.001	0.97
Diabetes	0.084	0.03	-0.005	0.93	-0.009	0.79	-0.065	0.054
Hyperlipidemia	0.029	0.48	-0.004	0.94	-0.002	0.96	-0.053	0.17
Smoking	0.037	0.45	-0.022	0.73	-0.041	0.30	-0.030	0.41
Atrial fibrillation	-0.061	0.13	-0.085	0.13	-0.027	0.44	-0.141	< 0.01
Coronary artery disease	0.029	0.47	-0.066	0.25	-0.029	0.41	-0.022	0.52
Left ventricular hypertrophy	0.038	0.33	0.008	0.88	0.079	0.02 [†]	0.045	0.17
Total cholesterol	-0.024	0.55	0.022	0.71	-0.027	0.46	0.061	0.08
Prior statin use	0.023	0.57	-0.149	0.01	-0.015	0.70	-0.059	0.14

*White matter hyperintensity (WMH) volumes were transformed to a logarithmic scale.

Supplemental Table VI. Literature review on white matter hyperintensity volume: comparison with the present study

Author	Population	Ethnicity	Mean age	Prevalence of Hypertension	Unit	Mean	Median	SD	IQR	Year	No. subjects
Jimenez-Conde et al. ²⁸	Ischemic stroke	Not reported	65	62	cm ³		8.0		3.9-16.2	2010	631
Schwartz et al. ¹⁴	General population without stroke	White (US)	63	84	cm ³	6.3			4.8-9.5	2007	343
Schwartz et al. ²⁹	General population without stroke	Black (US)	63	77	cm ³	6.9			4.9-9.9	2007	257
Rost et al. ³¹	Ischemic stroke	Not reported (US)	65	71	cm ³		6.9		3.1-11.9	2010	120
Rost et al. ²⁹	Ischemic stroke	Not reported (US)	65	62	cm ³	8.2			4.2-16.3	2010	523
Rost et al. ¹⁵	Ischemic and hemorrhagic stroke	Almost white* (US)	65	65	cm ³		7.5		3.4-14.7	2010	628
<i>Ryu et al. (present study)</i>	<i>Ischemic stroke</i>	<i>Asian (Korea)</i>	<i>67</i>	<i>66</i>	<i>cm³</i>		<i>7.3</i>		<i>3.5-15.3</i>	<i>2014</i>	<i>2669</i>
Russo et al. ³²	General population without stroke	Mainly Hispanic [†] (US)	69	73	%	0.6	0.3	0.9	0.5	2013	439
Gardener et al. ³³	General population without stroke	Mainly Hispanic [‡] (US)	72	Not reported	%	0.7		0.8		2012	966
Hoth et al. ⁸	General population with cardiovascular disease	Not reported (US)	73	76	%	0.7		1.2		2007	25
<i>Ryu et al. (present study)</i>	<i>Ischemic stroke</i>	<i>Asian (Korea)</i>	<i>67</i>	<i>67</i>	<i>%</i>	<i>1.0</i>	<i>0.6</i>	<i>1.1</i>	<i>0.3 - 1.3</i>	<i>2014</i>	<i>2669</i>

SD indicates standard deviation; and IQR, interquartile range.

Considering that the reported mean brain volume of an elderly Korean population was 1170cm³,³⁴ and assuming a uniform distribution of disease, white matter hyperintensity volume was calculated.

*>95% of subjects were White.

[†]70% were Hispanic, 13% White, and 16% Black.

[‡]65% were Hispanic, 16% White, and 18% Black.

Supplemental Table VII. A modified version of the Supplemental Table I, with the literature summary reorganized based on the mean age and prevalence of hypertension, for comparison with the present study

Author	Population	Mean age	Prevalence of HT	Relation with White Matter Hyperintensity Volume									
				Age	Sex, male	DM	HL	Smoking	Af	CAD	LVH	Cholesterol	
<i>Ryu et al. (Present study)</i>	<i>Younger non-hypertensive subgroup of ischemic stroke patients</i>	55	0	Positive	No	Positive	No	No	No	No	No	No	No
Schmidt et al. ^{22†}	General population with or without stroke	55	35	Positive	No	Positive	NA	NA	NA	No	NA	NA	NA
Awad et al. ²¹	General population with or without stroke	64	40	Positive	No	No	NA	NA	NA	No	NA	NA	NA
Jeerakathil et al. ^{26*}	General population without stroke	62	18	Positive	No	No	NA	Positive	NA	Positive	Positive	NA	NA
<i>Ryu et al. (Present study)</i>	<i>Younger hypertensive subgroup of ischemic stroke patients</i>	59	100	Positive	No	No	No	No	No	No	Positive	No	No
Schwartz et al. ^{14*}	General population without stroke	63	81	Positive	No	No	NA	No	NA	No	NA	NA	NA
Jimenez-Conde et al. ^{28†}	Ischemic stroke	65	62	Positive	No	No	Negative	No	No	No	NA	NA	NA
Rost et al. ^{29*}	Ischemic stroke	65	62	Positive	No	No	No	NA	Positive	Positive	NA	NA	NA
<i>Ryu et al. (Present study)</i>	<i>Older non-hypertensive subgroup of ischemic stroke patients</i>	77	0	Positive	No	No	No	No	No	No	No	No	No
Ylikoski et al. ^{23†}	General population without stroke	72	28	Positive	No	No	NA	NA	NA	NA	NA	NA	NA
Hirono et al. ²⁵	Demented patients with or without stroke	74	30	Positive	No	No	No	No	NA	No	NA	NA	NA
Longstreth et al. ¹³	General population without stroke	75	45	Positive	Negative	NA	NA	Positive	NA	Positive	NA	NA	NA
<i>Ryu et al. (Present study)</i>	<i>Older hypertensive subgroup of ischemic stroke patients</i>	78	100	Positive	No	Negative	Negative	No	Negative	No	No	No	Negative
Khan et al. ²⁷	Ischemic stroke [‡]	69	89	Positive	No	Negative	Negative	No	NA	Negative	NA	NA	NA
Jimenez-Conde et al. ^{28*}	Ischemic stroke	69	67	Positive	Negative	No	Negative	No	Negative	No	NA	NA	NA
Rostrup et al. ^{30*}	General population with or without stroke [§]	74	70	Positive	Positive	No	NA	Positive	NA	NA	NA	NA	No

Red-colored cell, a positive association between the variable and white matter hyperintensity (WMH); Green-colored cell, a negative association; Light gray-colored cell, no association; White-colored cell, not applicable (NA).

HT, hypertension; BMI, body mass index; DM, diabetes; HL, hyperlipidemia; Af, atrial fibrillation; CAD, coronary artery disease; LVH, left ventricular hypertrophy

*WMH volume was quantitatively measured.

†HT was not associated with WMHs.

‡Lacunar stroke

§Some patients with minor focal cerebrovascular events were enrolled.

Supplemental Table VIII. Patient characteristics: comparison between two different magnetic field strengths (1.5 Tesla vs. 3.0 Tesla)

	1.5 Tesla (n = 2,338)	3.0 Tesla (n = 331)	<i>P</i> *
Age, years	66.8 ± 13.0	66.9 ± 12.6	0.29
Sex, men	1394 (60%)	195 (59%)	0.81
Hypertension	1525 (65%)	238 (72%)	0.02
Diabetes	734 (31%)	113 (34%)	0.32
Hyperlipidemia	896 (38%)	107 (32%)	0.04
Smoking, current or quit < 5years	948 (41%)	167 (51%)	<0.01
Atrial fibrillation	484 (21%)	59 (18%)	0.22
Coronary artery disease	252 (11%)	59 (18%)	< 0.01
Body mass index, kg/m ²	23.5 ± 3.3	23.7 ± 3.3	0.84
Prior use of anti-platelet	487 (21%)	97 (29%)	<0.01
Prior use of statin	222 (10%)	51 (15%)	<0.01
Stroke subtype			
Large artery disease	891 (39%)	121 (37%)	0.02
Small vessel occlusion	385 (17%)	69 (21%)	
Cardioembolism	469 (21%)	81 (25%)	
Undetermined	509 (22%)	55 (17%)	
Other-determined	57 (3%)	4 (1%)	
NIHSS, median (IQR)	4 (2-9)	3 (2-5)	< 0.01 [†]
Left ventricular hypertrophy	294 (13%)	60 (18%)	< 0.01
Total cholesterol, mmol/l	4.68 ± 1.07	4.58 ± 1.12	0.30
HDL cholesterol, mmol/l	1.16 ± 0.32	1.14 ± 0.31	0.80
LDL cholesterol, mmol/l	2.94 ± 0.94	2.90 ± 0.98	0.26
Hemoglobin, g/dl	13.6 ± 2.0	13.6 ± 2.1	0.95
Glucose, mmol/l	6.45 ± 2.63	6.16 ± 1.98	0.04
HbA1c, %	6.46 ± 1.46	6.49 ± 1.44	0.91
Systolic blood pressure	146 ± 27	151 ± 28	0.24
Diastolic blood pressure	86 ± 16	84 ± 17	0.08
WMH volume, median (IQR)	0.61 (0.30-1.31)	0.64 (0.31-1.32)	0.90 [†]

To convert cholesterol to mg/dL, multiply values by 38.6.

To convert glucose to mg/dL, multiply values by 18.0.

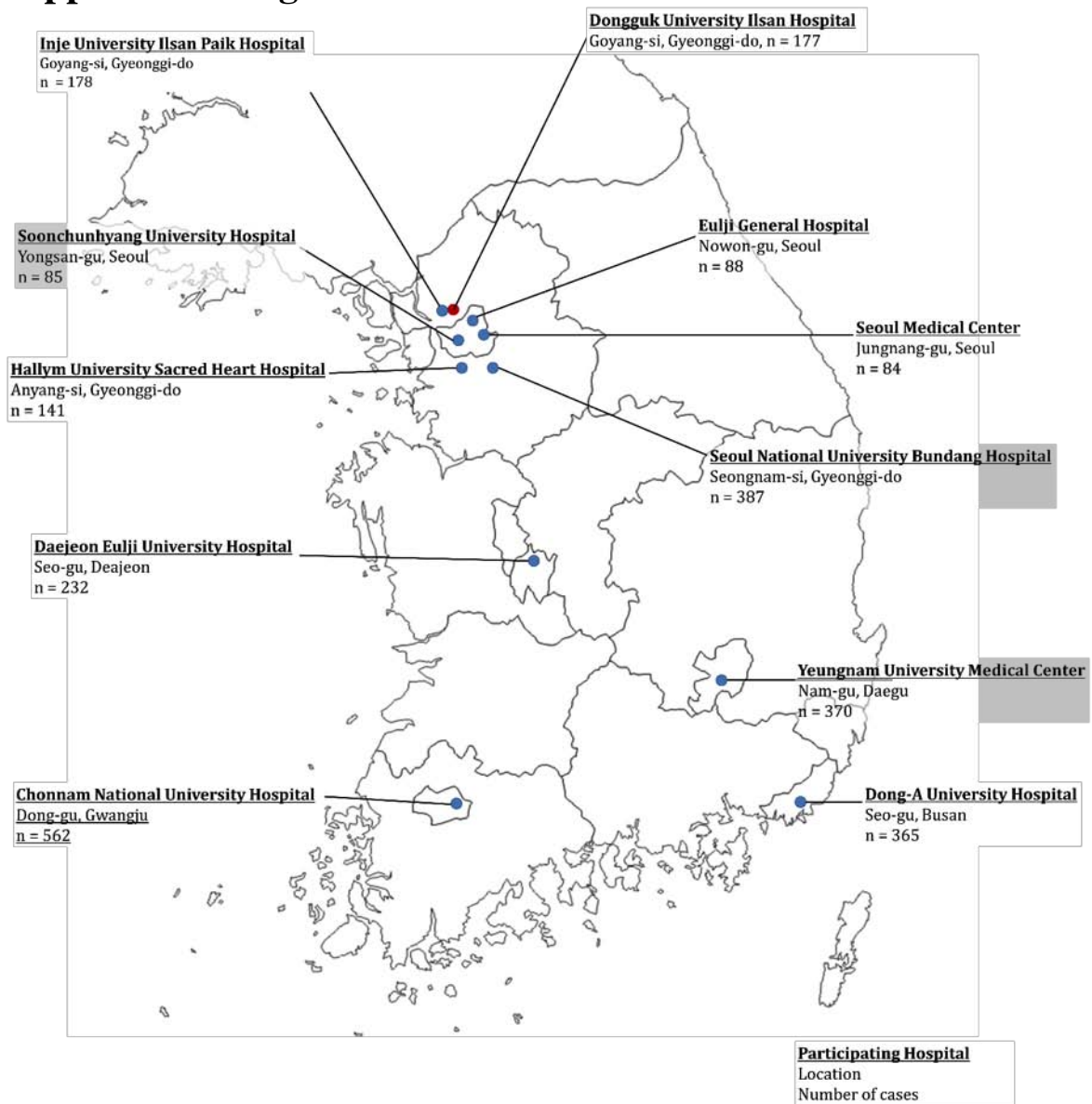
NIHSS, National Institutes of Health Stroke Scale; and IQR, interquartile range

Data are presented as number (percentage) or mean \pm standard deviation.

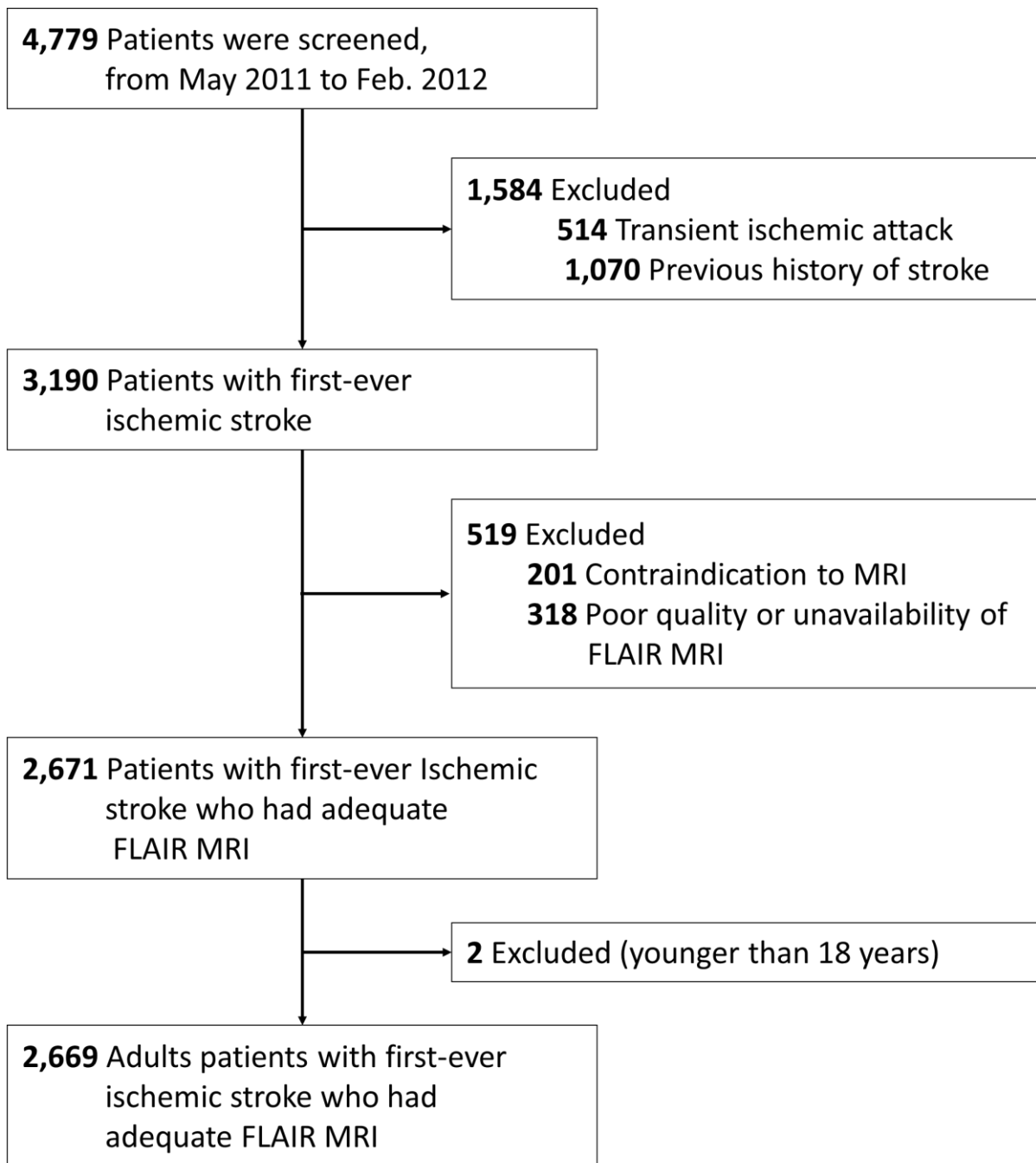
**P* values from Student *t*-test or chi-square test.

†Mann-Whitney *U* test was used.

Supplemental Figures



A. Distribution of Participating Centers

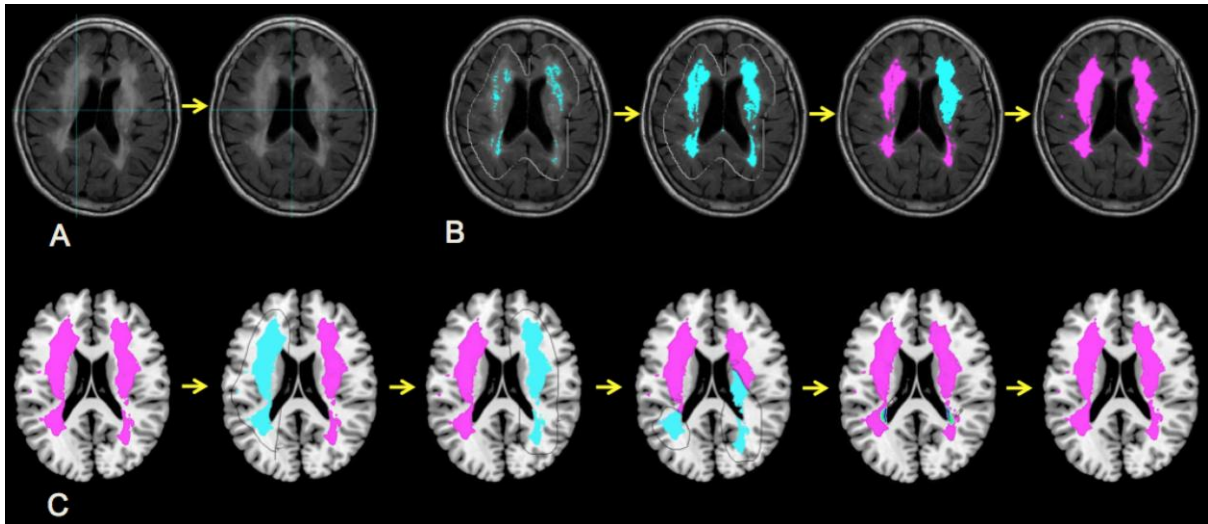


B. Study Flow Chart

Supplemental Figure I. Distribution of participating centers and enrollment of study subjects and study flow chart

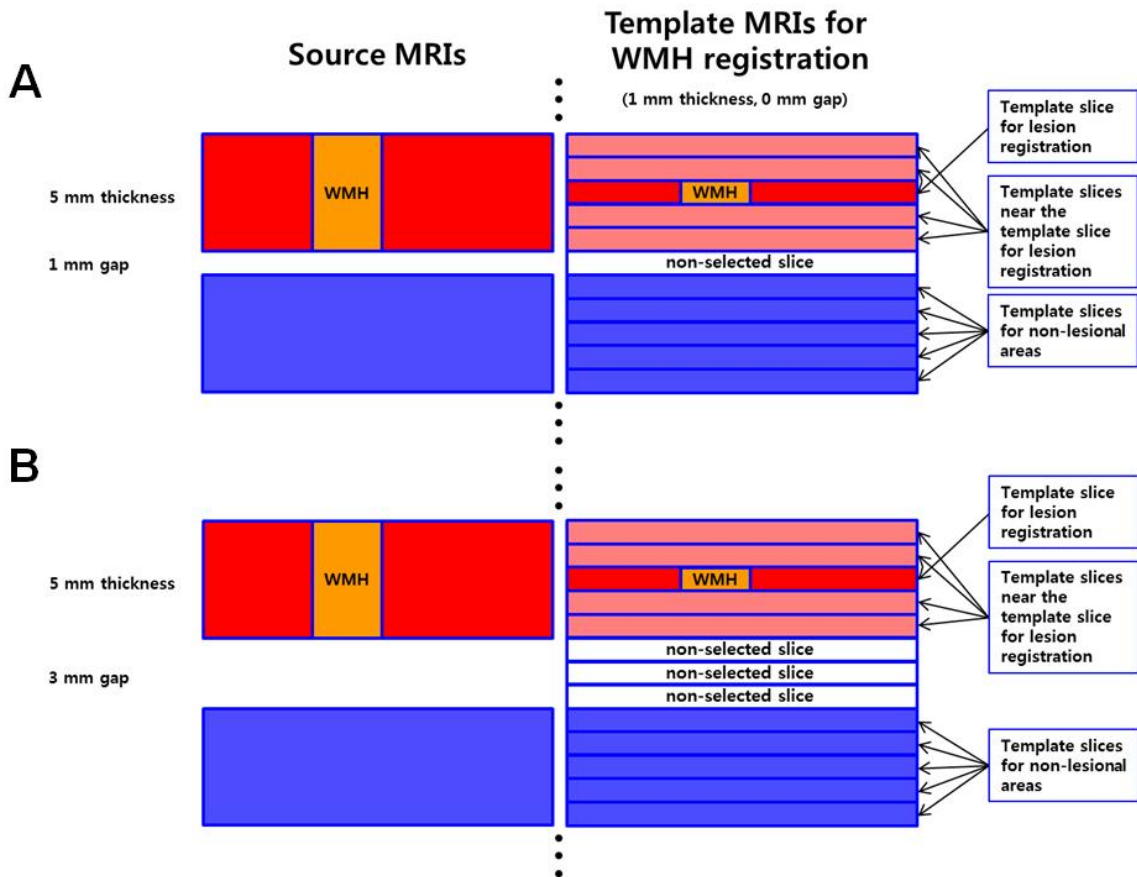
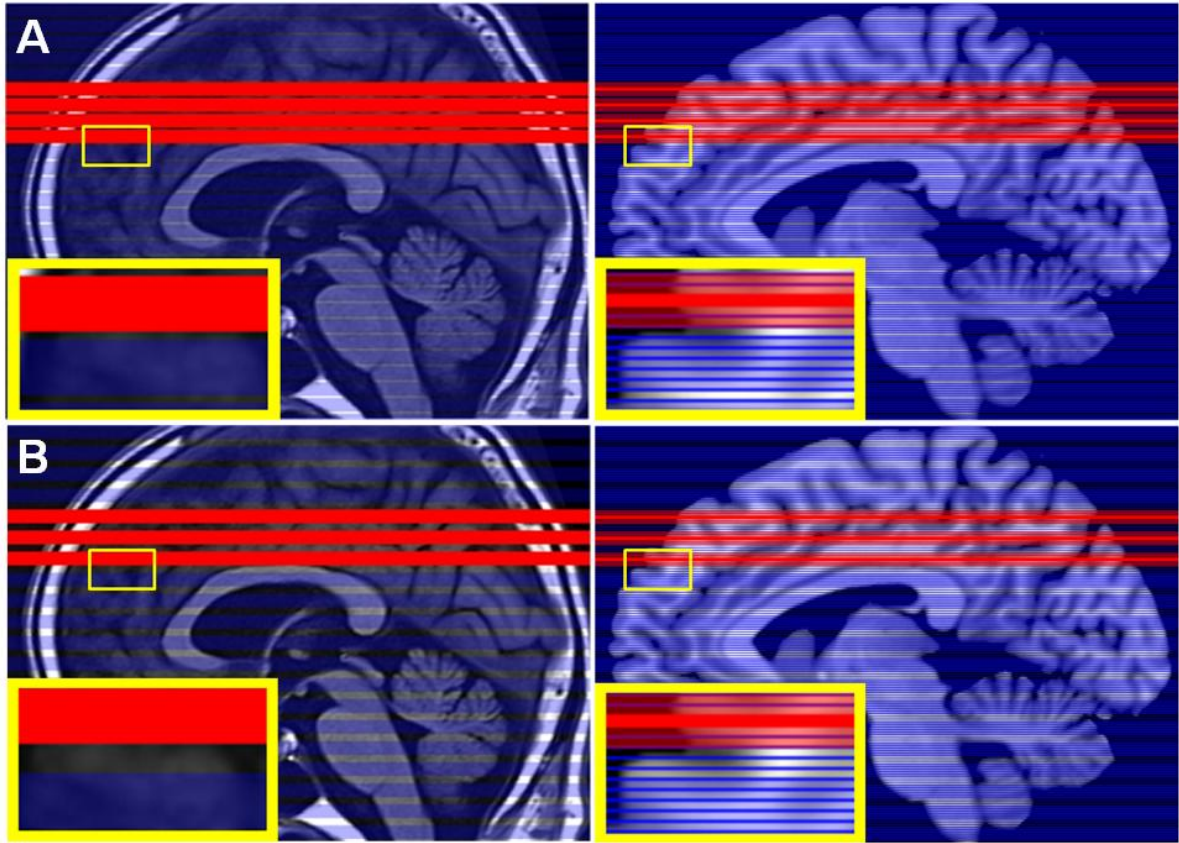
(A and B) After screening 4,799 acute (≤ 1 week) stroke patients from May-2011 to February-2012, a total of 2,699 first-ever ischemic stroke patients were enrolled consecutively from 11 centers participating in the Korean Nationwide Image-based Stroke Database Project,⁵ which is run by Korean Brain MRI Data Center (a National Center for Standard Reference Data at Dongguk University Ilsan Hospital) in collaboration with the Clinical Research Center for Stroke. The participating academic and regional stroke centers

represent each region of Korea, approximately reflecting the size of the entire Korean population of 50 million. Each center routinely (in >90% of cases) uses diffusion-weighted MRI and MR angiography / computed tomography angiography to evaluate acute ischemic stroke.³⁵ This study adhered to the Standards for Reporting Vascular changes on neuroimaging (STRIVE), which are recent recommendations on neuroimaging standards for research into small vessel disease.³⁶ We excluded the following patients: 1) age younger than 18 years (n=2), 2) transient ischemic attack (n=514), 3) contraindication to MRI (n=201), or 4) poor quality or unavailability of FLAIR MRI (n=318) (B).



Supplemental Figure II. Registration of white matter hyperintensity lesions on the template using a custom-built software package

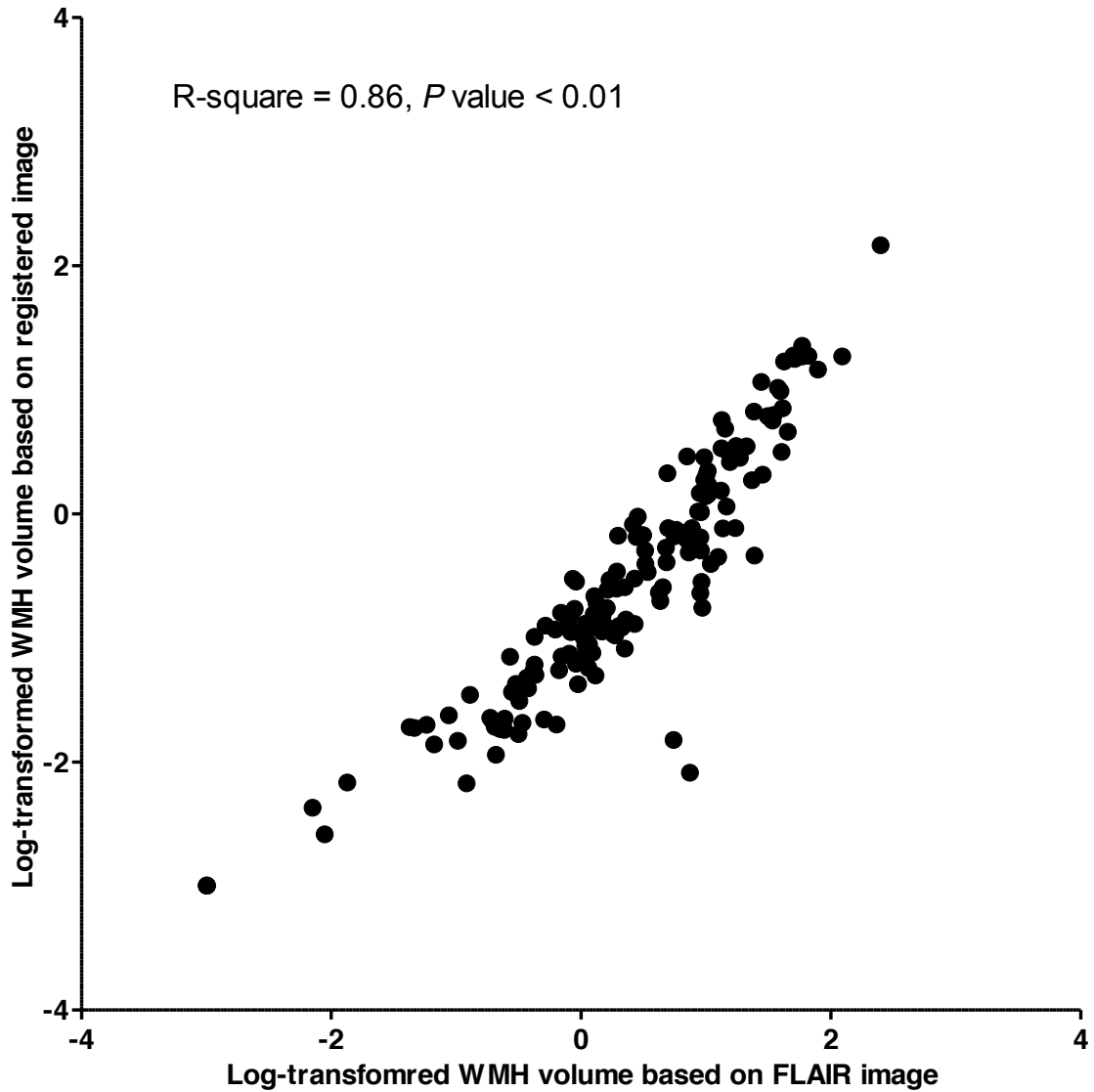
(A) A patient's FLAIR MRI is loaded, and normalized to give the background a 'gray scale pixel intensity' of 0. The image is then rotated so that the inter-hemispheric fissure is vertical. (B) The rater draws regions of interest (white circle) to encircle WMH lesion, and clicks on any pixel inside the lesion. The WMH area is selected automatically and colored pink by the software. The pink selection is then adjusted by excluding or including additional pixels of similar signal intensity range by rolling the wheel of the computer mouse up or down. (C) The adjusted area is automatically transferred to the Montreal Neurological Institute brain template using a mesh-warping algorithm and linear interpolation. Then, the rater makes final adjustments to the location and size of the WMH area to match the original source image as closely as possible.



Estimation of WMH volume % in the registration data = $100 \times \sum (\text{yellow registered lesion} \times 5 / \text{brain parenchyma in 10 red or blue slices})$

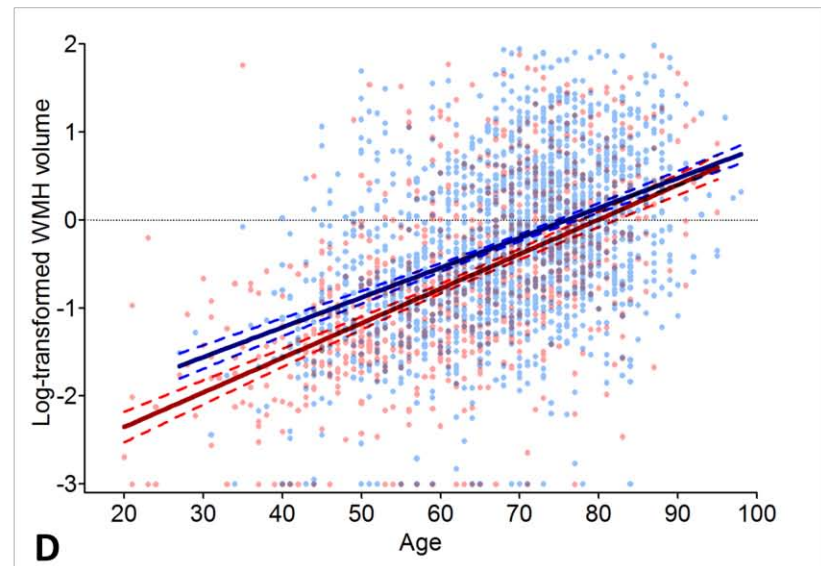
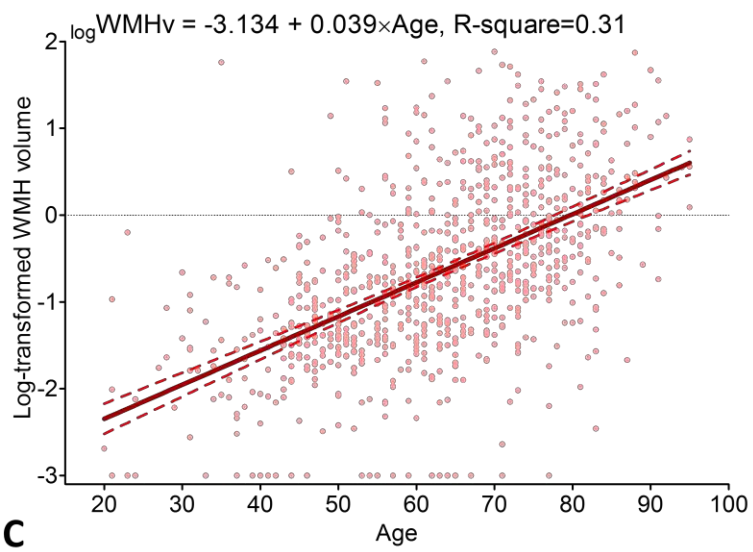
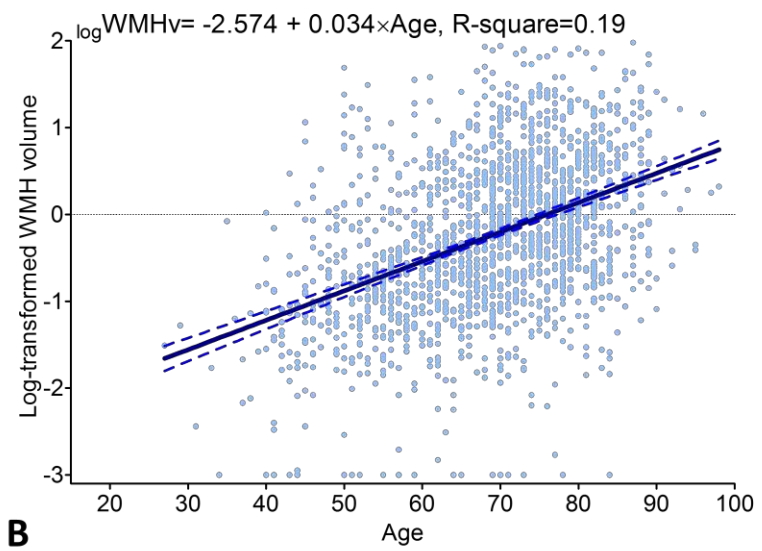
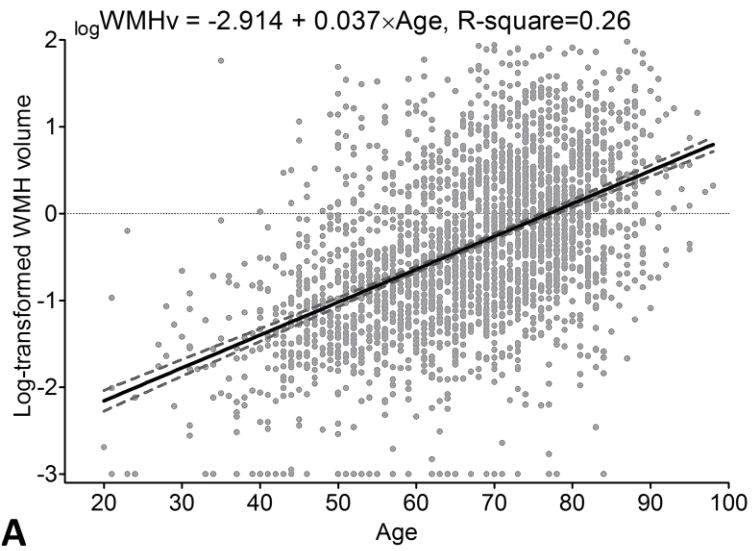
Supplemental Figure III. Estimation of white matter hyperintensity volume percentages while adjusting for the effects of different spacing of source MRIs and template images

A (upper figure) and **B** (lower figure). Source MRI are in the left column, and template images are in the right column. The bright red color indicates WMH lesion-containing source MRI slices or template MRI slices with registered lesions; light blue colored source MRI slices have no lesions, and light blue template MRI slices are similarly without lesions. The light red colored template MRI sections are clustered around the template slice containing the registered lesion, and indicate slices that might not be counted as abnormal, due to a mismatch in slice thicknesses between the source and template images. For lesion volume calculations to be accurate, the total thickness of the bright red-colored plus the light red-colored template MRI slices needs to be equal to that of the red-colored source MR slices. Σ indicates summation of the entire whole brain dataset (except for the interslice gaps). Inlets (in B) are for a magnified view of a single imaging section. Because the slice thickness of the template is 1 mm, a white matter lesion detected inside a 5 mm thick clinical scan would map to a single 1 mm template slice, falsely undercounting the lesion volume by a factor of 5. The nearby template slices indicated by light red coloring should have been included in lesion volume calculation, while excluding blue non-lesion containing slices. To balance this out, the quantitation of WMH volume in the template should be multiplied by a factor of 5. Also note the ambiguity introduced by the interslice gap; in the case of a scan with a larger (3 mm) interslice gap, compared with a smaller (1 mm) interslice gap, the total brain volume calculated using the source MRI decreases. The same patient scanned two different ways would have a lower WMH lesion percentage in the top set of images, than in the lower set of images. To counteract this effect, the template slices that fall between the lesional (red color) and non-lesional (light blue color) scan slices are excluded (= non-selected slices in the Figure) in the calculation of WMH volume percentage. Therefore, the total numbers of brain parenchymal voxels used in the denominator for WMH volume calculations varied from 806,611 to 2,155,881, depending on the slice thickness (3 - 7 mm) and inter-slice gap (2.5 - 0 mm) of each center's MRI (see Table III in the online only Data Supplement for specifics). This adjustment ensures that the percentage WMH remains invariant with scanning technique. Please note that in every patient of this study (n = 2,699), all, that is the complete brain data set, including all 'lesion-positive and lesion-negative' FLAIR MRIs (usually 20 ~ 26 5mm-thick slices per patient) were used for WMH segmentation and registration onto the Montreal Neurologic Institute (MNI) template. Thus, WMH quantification was based on an assessment of the entire brain volume in every patient.



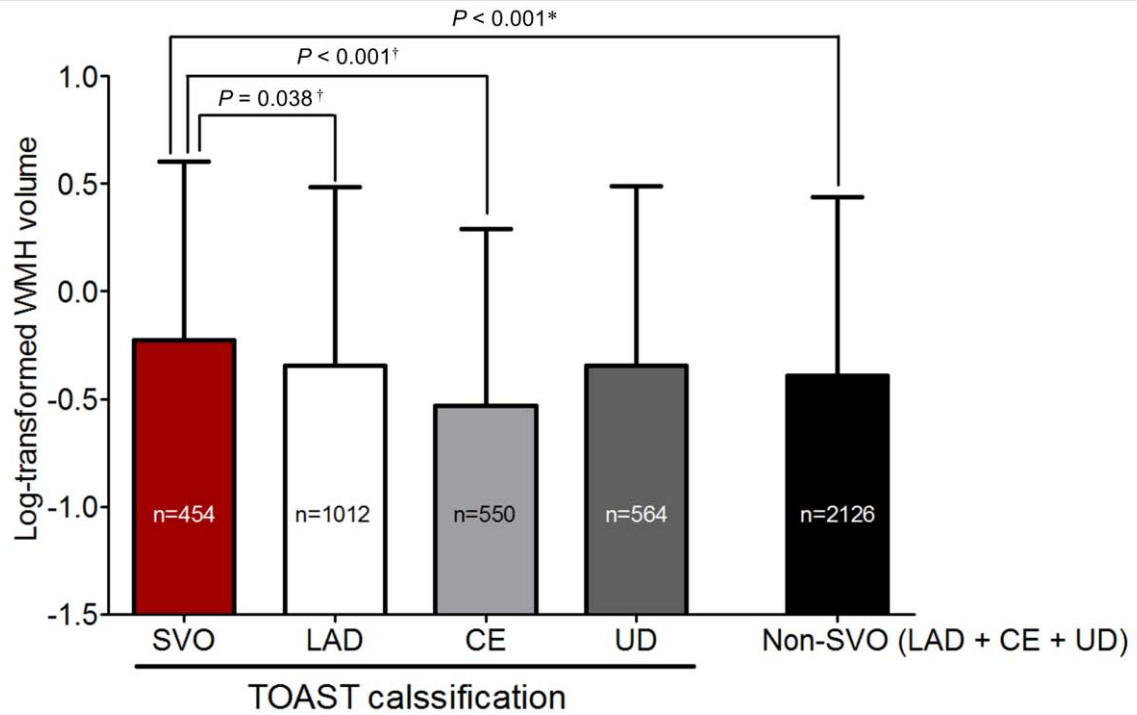
Supplemental Figure IV. Correlation between white matter hyperintensity (WMH) volume calculations in the template image space (used for the lesion registration and quantification for the main studies) and WMH volume calculations done in the original FLAIR MRI space

Because of the skewed distribution of WMH volumes, log-transformed data are presented. Each dot represents one patient's WMH volume.



Supplemental Figure V. Scatter plots and linear regressions (equations and R-square on figures) to show the age / hypertension-dependence of white matter hyperintensity volume

A. All patients, **B.** Hypertensive patients, **C.** Non-hypertensive patients, and **D.** Overlay of B (blue line) and C (red line). Please note that the blue line approaches the red line as age increases, indicating the presence of an interaction between age and hypertension. Dots indicate log-transformed WMH volumes of individual patients. Solid line and light-colored area represent linear regression line and 95% confidence interval, respectively. WMH volumes were transformed to a logarithmic scale by using the equation $\log(\text{WMH volume} + 0.05)$ after considering that the frequency distribution of WMH volumes was skewed and some patients had no WMH.



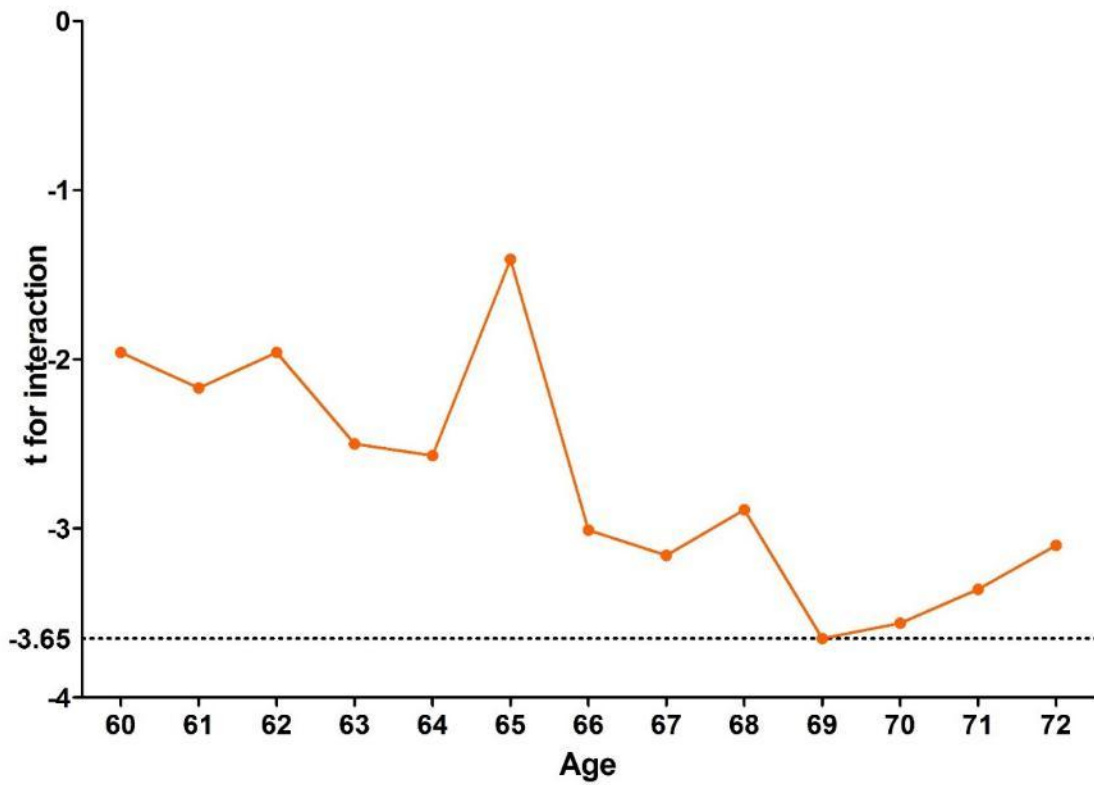
Supplemental Figure VI. Age-adjusted white matter hyperintensity volumes in different stroke subtypes

Age-adjusted \log_{10} WMHv was calculated by using marginal linear prediction after ANOVA, followed by pairwise comparison with a Bonferroni correction.

WMH, white matter hyperintensities; SVO, small vessel occlusion; LAD, large artery disease; CE, cardioembolism; UD, undetermined etiology; TOAST, Trial of Org 10172 in Acute Stroke Treatment.

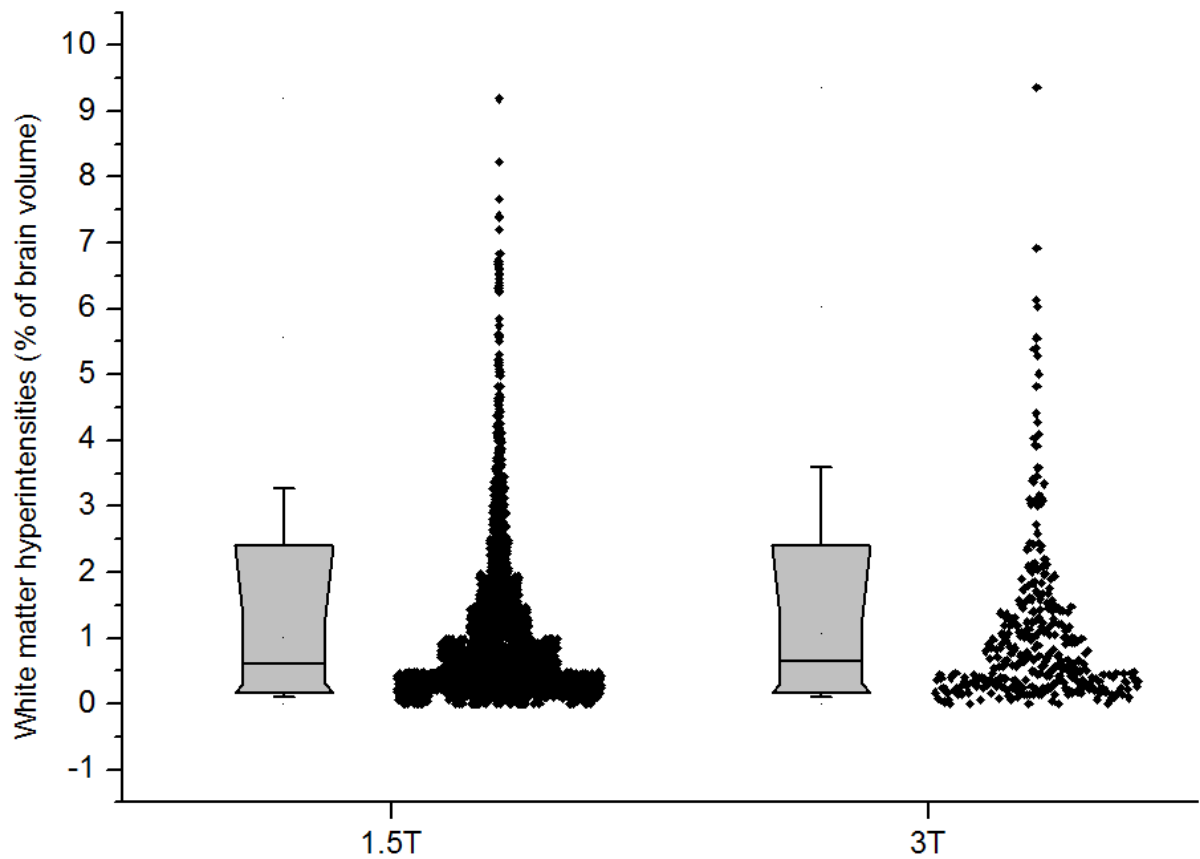
*Student t-test was used.

†Pairwise comparison with a Bonferroni correction



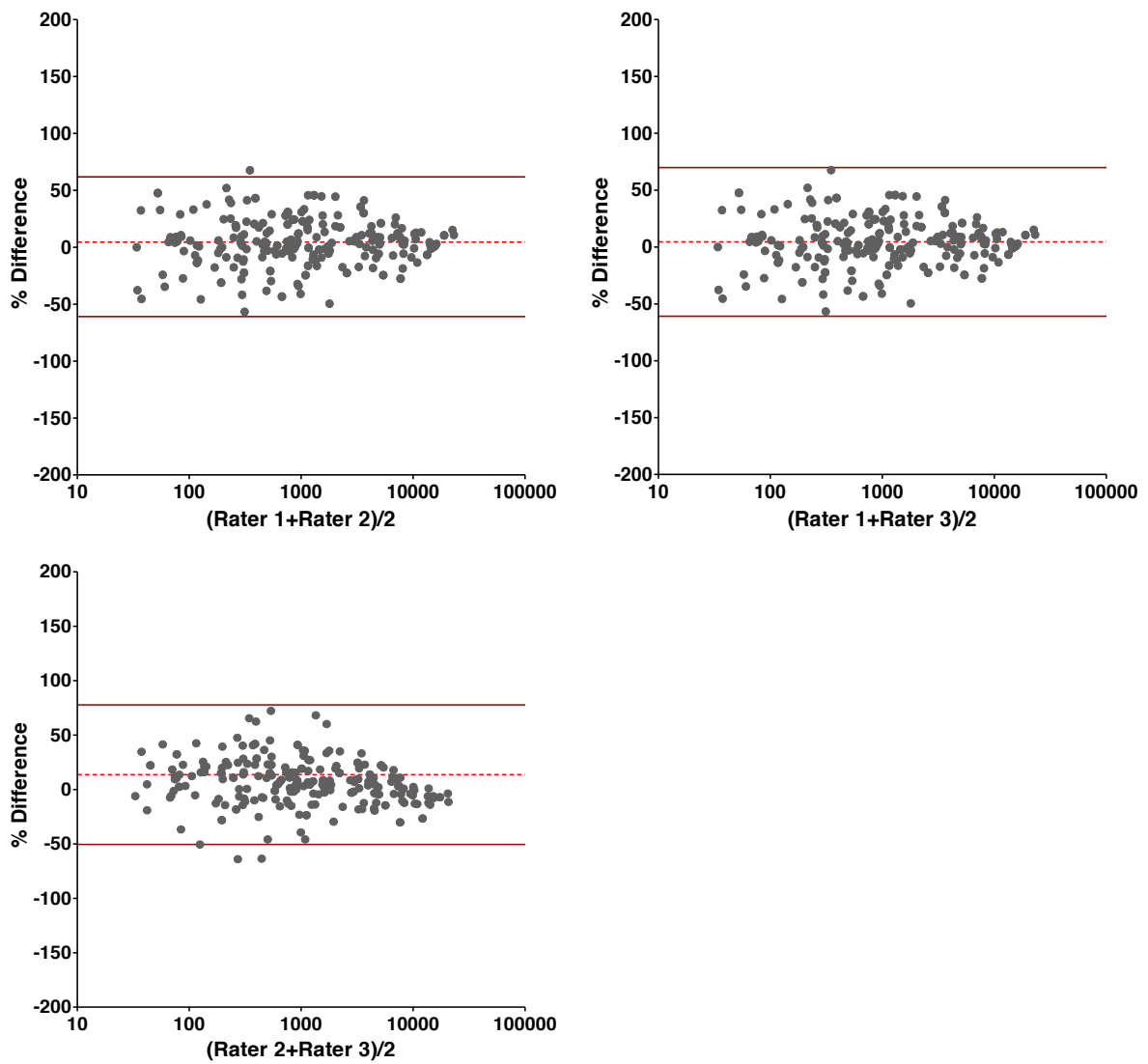
Supplemental Figure VII. t-values for interaction between hypertension and dichotomized age

X-axis values indicate the age of dichotomization. When age is dichotomized at 69 years, t-value becomes the lowest ($t = -3.65$, $P < 0.01$).



Supplemental Figure VIII. Box plots with scatter plots for white matter hyperintensities: comparison between two different magnetic field strengths (1.5T vs. 3T)

The lower and upper horizontal bars outside each box represent 5% and 95% of the data. The middle line in the box represents the median value of the data (50%), while the lower and upper border of the box represent 25% and 75% of the data, respectively. There are no significant differences in WMH volumes between these two groups (Mann-Whitney U -test, $P = 0.61$).



Supplemental Figure IX. Inter-rater reliability of the measurement of white matter hyperintensity volume

In the Bland-Altman plots, red dashed and solid lines represent mean difference and 95% limits of agreement, respectively. There is a high level of agreement between three raters.

Supplemental Video. Examples of using the new visual grading system for white matter hyperintensity

The video illustrates examples of using the well-known Fazekas scale vs. our new age-adjusted WMH-grading system that reflects the topographic statistical prevalence of WMHs in a stroke population.

Supplementary References

1. Whitworth JA; World Health Organization, International Society of Hypertension Writing Group. 2003 World Health Organization (WHO)/International Society of Hypertension (ISH) statement on management of hypertension.. *J Hypertens*. 2003;21:1983-1992.
2. American Diabetes Association. Diagnosis and classification of diabetes mellitus. *Diabetes Care*. 2011;34 Suppl 1:S62-69.
3. National Cholesterol Education Program (NCEP) Expert Panel on Detection, Evaluation, and Treatment of High Blood Cholesterol in Adults (Adult Treatment Panel III). Third Report of the National Cholesterol Education Program (NCEP) Expert Panel on Detection, Evaluation, and Treatment of High Blood Cholesterol in Adults (Adult Treatment Panel III) final report. *Circulation*. 2002;106:3143-3421.
4. Adams HP, Jr., Woolson RF, Clarke WR, Davis PH, Bendixen BH, Love BB, et al. Design of the Trial of Org 10172 in Acute Stroke Treatment (TOAST). *Control Clin Trials*. 1997;18:358-377.
5. Kim DE, Park KJ, Schellingerhout D, Jeong SW, Ji MG, Choi WJ, et al. A new image-based stroke registry containing quantitative magnetic resonance imaging data. *Cerebrovasc Dis*. 2011;32:567-576.
6. Lim JS, Kim N, Jang MU, Han MK, Kim S, Baek MJ, et al. Cortical hubs and subcortical cholinergic pathways as neural substrates of poststroke dementia. *Stroke*. 2014;45:1069-1076.
7. Ay H, Arsava EM, Rosand J, Furie KL, Singhal AB, Schaefer PW, et al. Severity of leukoaraiosis and susceptibility to infarct growth in acute stroke. *Stroke*. 2008;39:1409-1413.
8. Hoth KF, Tate DF, Poppas A, Forman DE, Gunstad J, Moser DJ, et al. Endothelial function and white matter hyperintensities in older adults with cardiovascular disease. *Stroke*. 2007;38:308-312.
9. Kim DE, Kim JY, Schellingerhout D, Kim EJ, Kim HK, Lee S, et al. Protease imaging of human atheromata captures molecular information of atherosclerosis, complementing anatomic imaging. *Arterioscler Thromb Vasc Biol*. 2010;30:449-456.
10. Kim DE, Kim JY, Nahrendorf M, Lee SK, Ryu JH, Kim K, et al. Direct thrombus imaging as a means to control the variability of mouse embolic infarct models: the role of optical molecular imaging. *Stroke*. 2011;42:3566-3573.
11. Basile AM, Pantoni L, Pracucci G, Asplund K, Chabriat H, Erkinjuntti T, et al. Age, hypertension, and lacunar stroke are the major determinants of the severity of age-related white matter changes. The LADIS (Leukoaraiosis and Disability in the Elderly) Study. *Cerebrovasc Dis*. 2006;21:315-322.
12. de Leeuw FE, de Groot JC, Oudkerk M, Kors JA, Hofman A, van Gijn J, et al. Atrial fibrillation and the risk of cerebral white matter lesions. *Neurology*. 2000;54:1795-1801.
13. Lindgren A, Roijer A, Rudling O, Norrving B, Larsson EM, Eskilsson J, et al. Cerebral lesions on magnetic resonance imaging, heart disease, and vascular risk factors in subjects without stroke. A population-based study. *Stroke*. 1994;25:929-934.

14. Schwartz GL, Bailey KR, Mosley T, Knopman DS, Jack CR, Jr., Canzanello VJ, et al. Association of ambulatory blood pressure with ischemic brain injury. *Hypertension*. 2007;49:1228-1234.
15. Rost NS, Rahman RM, Biffi A, Smith EE, Kanakis A, Fitzpatrick K, et al. White matter hyperintensity volume is increased in small vessel stroke subtypes. *Neurology*. 2010;75:1670-1677.
16. Williams R. Using the margins command to estimate and interpret adjusted predictions and marginal effects. *The Stata Journal*. 2012;12:308-331.
17. Debette S, Markus HS. The clinical importance of white matter hyperintensities on brain magnetic resonance imaging: systematic review and meta-analysis. *BMJ*. 2010;341:c3666.
18. Carmelli D, DeCarli C, Swan GE, Jack LM, Reed T, Wolf PA, et al. Evidence for genetic variance in white matter hyperintensity volume in normal elderly male twins. *Stroke*. 1998;29:1177-1181.
19. Chung MK, Robbins S, Evans AC. Unified statistical approach to cortical thickness analysis. *Inf Process Med Imaging*. 2005;19:627-638.
20. Lee JE, Chung MK, Lazar M, DuBray MB, Kim J, Bigler ED, et al. A study of diffusion tensor imaging by tissue-specific, smoothing-compensated voxel-based analysis. *Neuroimage*. 2009;44:870-883.
21. Awad IA, Spetzler RF, Hodak JA, Awad CA, Carey R. Incidental subcortical lesions identified on magnetic resonance imaging in the elderly. I. Correlation with age and cerebrovascular risk factors. *Stroke*. 1986;17:1084-1089.
22. Schmidt R, Fazekas F, Kleinert G, Offenbacher H, Gindl K, Payer F, et al. Magnetic resonance imaging signal hyperintensities in the deep and subcortical white matter. A comparative study between stroke patients and normal volunteers. *Arch Neurol*. 1992;49:825-827.
23. Ylikoski A, Erkinjuntti T, Raininko R, Sarna S, Sulkava R, Tilvis R. White matter hyperintensities on mri in the neurologically nondiseased elderly. Analysis of cohorts of consecutive subjects aged 55 to 85 years living at home. *Stroke*. 1995;26:1171-1177.
24. Longstreth WT, Jr., Manolio TA, Arnold A, Burke GL, Bryan N, Jungreis CA, et al. Clinical correlates of white matter findings on cranial magnetic resonance imaging of 3301 elderly people. The Cardiovascular Health Study. *Stroke*. 1996;27:1274-1282.
25. Hirono N, Yasuda M, Tanimukai S, Kitagaki H, Mori E. Effect of the apolipoprotein E epsilon4 allele on white matter hyperintensities in dementia. *Stroke*. 2000;31:1263-1268.
26. Jeerakathil T, Wolf PA, Beiser A, Massaro J, Seshadri S, D'Agostino RB, et al. Stroke risk profile predicts white matter hyperintensity volume: the Framingham Study. *Stroke*. 2004;35:1857-1861.
27. Khan U, Porteous L, Hassan A, Markus HS. Risk factor profile of cerebral small vessel disease and its subtypes. *J Neurol Neurosurg Psychiatry*. 2007;78:702-706.
28. Jimenez-Conde J, Biffi A, Rahman R, Kanakis A, Butler C, Sonni S, et al. Hyperlipidemia and reduced white matter hyperintensity volume in patients with ischemic stroke. *Stroke*. 2010;41:437-442.
29. Rost NS, Rahman R, Sonni S, Kanakis A, Butler C, Massasa E, et al. Determinants of white matter hyperintensity volume in patients with acute ischemic stroke. *J Stroke Cerebrovasc Dis*. 2010;19:230-235.
30. Rostrup E, Gouw AA, Vrenken H, van Straaten EC, Ropele S, Pantoni L, et al. The spatial distribution of age-related white matter changes as a function of vascular risk

- factors--results from the LADIS study. *Neuroimage*. 2012;60:1597-1607.
31. Rost NS, Fitzpatrick K, Biffi A, Kanakis A, Devan W, Anderson CD, et al. White matter hyperintensity burden and susceptibility to cerebral ischemia. *Stroke*. 2010;41:2807-2811.
 32. Russo C, Jin Z, Homma S, Elkind MS, Rundek T, Yoshita M, et al. Subclinical left ventricular dysfunction and silent cerebrovascular disease: the Cardiovascular Abnormalities and Brain Lesions (CABL) study. *Circulation*. 2013;128:1105-1111.
 33. Gardener H, Scarmeas N, Gu Y, Boden-Albala B, Elkind MS, Sacco RL, et al. Mediterranean diet and white matter hyperintensity volume in the Northern Manhattan Study. *Arch Neurol*. 2012;69:251-256.
 34. Kwon JY, Rhyu IJ, Cheon JJ, Koh IS. Brain volume measurement of healthy Korean for clinical application using MRI. *The Report of National Institute of Health*. 2001;38:279-284.
 35. Kim BJ, Han MK, Park TH, Park SS, Lee KB, Lee BC, et al. Current status of acute stroke management in Korea: a report on a multicenter, comprehensive acute stroke registry. *Int J Stroke*. 2014;9:514-518.
 36. Wardlaw JM, Smith EE, Biessels GJ, Cordonnier C, Fazekas F, Frayne R, et al. Neuroimaging standards for research into small vessel disease and its contribution to ageing and neurodegeneration. *Lancet Neurol*. 2013;12:822-838.